



# TECH BRIEFS

NATIONAL AERONAUTICS AND SPACE ADMINISTRATION

-  Technology Focus
-  Electronics/Computers
-  Software
-  Materials
-  Mechanics/Machinery
-  Manufacturing
-  Bio-Medical
-  Physical Sciences
-  Information Sciences
-  Books and Reports



## INTRODUCTION

Tech Briefs are short announcements of innovations originating from research and development activities of the National Aeronautics and Space Administration. They emphasize information considered likely to be transferable across industrial, regional, or disciplinary lines and are issued to encourage commercial application.

### Availability of NASA Tech Briefs and TSPs

Requests for individual Tech Briefs or for Technical Support Packages (TSPs) announced herein should be addressed to

#### National Technology Transfer Center

Telephone No. **(800) 678-6882** or via World Wide Web at <http://www.nttc.edu/about/contactus.asp>

Please reference the control numbers appearing at the end of each Tech Brief. Information on NASA's Innovative Partnerships Program (IPP), its documents, and services is also available at the same facility or on the World Wide Web at <http://ipp.nasa.gov>.

Innovative Partnerships Offices are located at NASA field centers to provide technology-transfer access to industrial users. Inquiries can be made by contacting NASA field centers listed below.

## NASA Field Centers and Program Offices

Ames Research Center  
Lisa L. Lockyer  
(650) 604-1754  
[lisa.l.lockyer@nasa.gov](mailto:lisa.l.lockyer@nasa.gov)

Dryden Flight Research Center  
Gregory Poteat  
(661) 276-3872  
[greg.poteat@dfrc.nasa.gov](mailto:greg.poteat@dfrc.nasa.gov)

Glenn Research Center  
Kathy Needham  
(216) 433-2802  
[kathleen.k.needham@nasa.gov](mailto:kathleen.k.needham@nasa.gov)

Goddard Space Flight Center  
Nona Cheeks  
(301) 286-5810  
[nona.k.cheeks@nasa.gov](mailto:nona.k.cheeks@nasa.gov)

Jet Propulsion Laboratory  
Ken Wolfenbarger  
(818) 354-3821  
[james.k.wolfenbarger@jpl.nasa.gov](mailto:james.k.wolfenbarger@jpl.nasa.gov)

Johnson Space Center  
Michele Brekke  
(281) 483-4614  
[michele.a.brekke@nasa.gov](mailto:michele.a.brekke@nasa.gov)

Kennedy Space Center  
David R. Makufka  
(321) 867-6227  
[david.r.makufka@nasa.gov](mailto:david.r.makufka@nasa.gov)

Langley Research Center  
Martin Waszak  
(757) 864-4015  
[martin.r.waszak@nasa.gov](mailto:martin.r.waszak@nasa.gov)

Marshall Space Flight Center  
Jim Dowdy  
(256) 544-7604  
[jim.dowdy@msfc.nasa.gov](mailto:jim.dowdy@msfc.nasa.gov)

Stennis Space Center  
John Bailey  
(228) 688-1660  
[john.w.bailey@nasa.gov](mailto:john.w.bailey@nasa.gov)

Carl Ray, Program Executive  
Small Business Innovation  
Research (SBIR) & Small  
Business Technology  
Transfer (STTR) Programs  
(202) 358-4652  
[carl.g.ray@nasa.gov](mailto:carl.g.ray@nasa.gov)

Doug Comstock, Director  
Innovative Partnerships  
Program Office  
(202) 358-2560  
[doug.comstock@nasa.gov](mailto:doug.comstock@nasa.gov)





# TECH BRIEFS

## NATIONAL AERONAUTICS AND SPACE ADMINISTRATION



### 5 Technology Focus: Sensors

- 5 Control Architecture for Robotic Agent Command and Sensing
- 6 Algorithm for Wavefront Sensing Using an Extended Scene
- 6 CO<sub>2</sub> Sensors Based on Nanocrystalline SnO<sub>2</sub> Doped With CuO
- 7 Improved Airborne System for Sensing Wildfires



### 9 Electronics/Computers

- 9 VHF Wide-Band, Dual-Polarization Microstrip-Patch Antenna
- 10 Onboard Data Processor for Change-Detection Radar Imaging
- 11 Using LDPC Code Constraints To Aid Recovery of Symbol Timing
- 12 System for Measuring Flexing of a Large Spaceborne Structure
- 12 Integrated Formation Optical Communication and Estimation System



### 13 Manufacturing & Prototyping

- 13 Making Superconducting Welds Between Superconducting Wires
- 13 Method for Thermal Spraying of Coatings Using Resonant-Pulsed Combustion



### 15 Materials

- 15 Coating Reduces Ice Adhesion
- 15 Hybrid Multifoil Aerogel Thermal Insulation



### 17 Software

- 17 SHINE Virtual Machine Model for In-flight Updates of Critical Mission Software
- 17 Mars Image Collection Mosaic Builder
- 17 Providing Internet Access to High-Resolution Mars Images
- 17 Providing Internet Access to High-Resolution Lunar Images
- 18 Expressions Module for the Satellite Orbit Analysis Program
- 18 Virtual Satellite
- 18 Small-Body Extensions for the Satellite Orbit Analysis Program (SOAP)
- 18 Scripting Module for the Satellite Orbit Analysis Program (SOAP)

19 XML-Based SHINE Knowledge Base Interchange Language

19 Core Technical Capability Laboratory Management System

20 MRO SOW Daily Script



### 21 Mechanics /Machinery

- 21 Tool for Inspecting Alignment of Twinaxial Connectors
- 22 An ATP System for Deep-Space Optical Communication
- 22 Polar Traverse Rover Instrument



### 23 Bio-Medical

- 23 Expert System Control of Plant Growth in an Enclosed Space
- 24 Detecting Phycocyanin-Pigmented Microbes in Reflected Light



### 25 Physical Science

- 25 DMAC and NMP as Electrolyte Additives for Li-Ion Cells
- 26 Mass Spectrometer Containing Multiple Fixed Collectors
- 27 Waveguide Harmonic Generator for the SIM
- 27 Whispering Gallery Mode Resonator With Orthogonally Reconfigurable Filter Function
- 27 Stable Calibration of Raman Lidar Water-Vapor Measurements
- 28 Bimaterial Thermal Compensators for WGM Resonators



### 31 Information Sciences

- 31 Root Source Analysis/ ValuStream™ — a Methodology for Identifying and Managing Risks
- 32 Ensemble: an Architecture for Mission-Operations Software
- 32 Object Recognition Using Feature-and Color-Based Methods



### 35 Books & Reports

- 35 On-Orbit Multi-Field Wavefront Control With a Kalman Filter
- 35 The Interplanetary Overlay Networking Protocol Accelerator

This document was prepared under the sponsorship of the National Aeronautics and Space Administration. Neither the United States Government nor any person acting on behalf of the United States Government assumes any liability resulting from the use of the information contained in this document, or warrants that such use will be free from privately owned rights.





## Control Architecture for Robotic Agent Command and Sensing

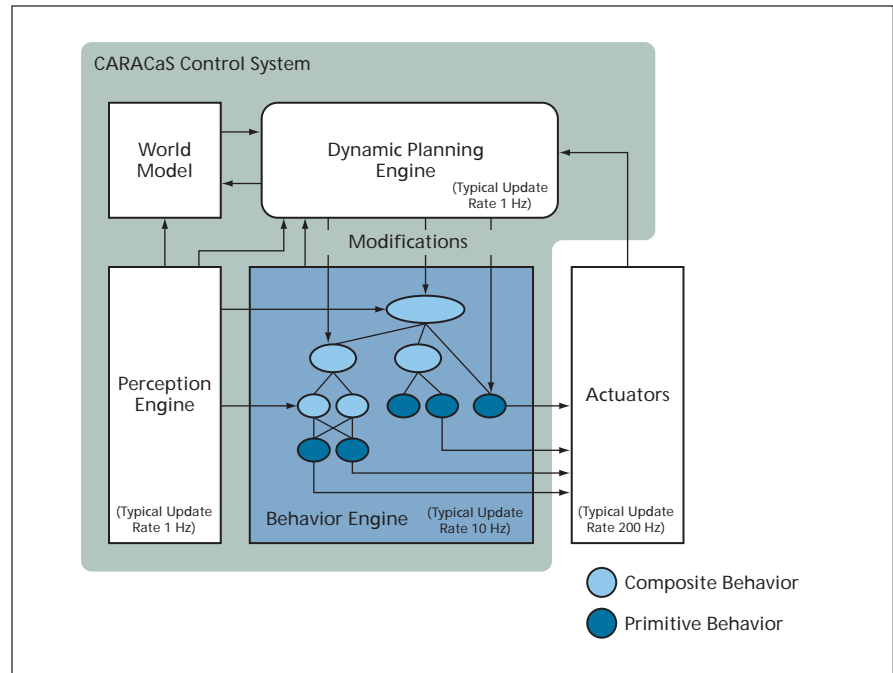
Plans and behaviors are updated in response to changing requirements and conditions.

NASA's Jet Propulsion Laboratory, Pasadena, California

Control Architecture for Robotic Agent Command and Sensing (CARACaS) is a recent product of a continuing effort to develop architectures for controlling either a single autonomous robotic vehicle or multiple cooperating but otherwise autonomous robotic vehicles. CARACaS is potentially applicable to diverse robotic systems that could include aircraft, spacecraft, ground vehicles, surface water vessels, and/or underwater vessels.

CARACaS (see figure) includes an integral combination of three coupled agents: a dynamic planning engine, a behavior engine, and a perception engine. The perception and dynamic planning engines are also coupled with a memory in the form of a world model. CARACaS is intended to satisfy the need for two major capabilities essential for proper functioning of an autonomous robotic system: a capability for deterministic reaction to unanticipated occurrences and a capability for re-planning in the face of changing goals, conditions, or resources.

The behavior engine incorporates the multi-agent control architecture, called "CAMPOUT," described in "An Architecture for Controlling Multiple Robots" (NPO-30345), *NASA Tech Briefs*, Vol. 28, No. 11 (November 2004), page 65. CAMPOUT is used to develop behavior-composition and -coordination mechanisms. Real-time process algebra operators are used to compose a behavior network for any given mission scenario. These operators afford a capability for producing a formally correct kernel of behaviors that guarantee predictable performance. By use of a method based on multi-objective decision theory (MODT), recommendations from multiple behaviors are combined to form a set of control actions that represents their consensus. In this approach, all behaviors contribute simultaneously to the control of the robotic system in a cooperative rather than a competitive manner. This approach guarantees a solution that is "good enough" with respect to resolution of complex, possibly conflicting goals within the constraints of the mission to be accom-



A CARACaS Control System includes three coupled agents (the engines) and a world model. The network in the behavior engine is built from primitive and composite behaviors. The dynamic planning engine interacts with the network at both the primitive and composite levels.

plished by the vehicle(s). CARACaS further uses another MODT-based method to systematically narrow the set of possible solutions, thereby producing an output within a time orders of magnitude shorter than would be necessary to compute a solution through brute-force search of the action space.

The dynamic planning engine incorporates the architecture embodied in the CASPER software, which was described in "Software for Continuous Replanning During Execution" (NPO-20972), *NASA Tech Briefs*, Vol. 26, No. 4 (April 2002), page 67. Given an input set of mission goals and the autonomous vehicle's current state, CASPER generates a plan of activities that satisfies as many goals as possible while still obeying relevant resource constraints and operation rules. Plans are dynamically updated by use of an iterative repair algorithm that classifies conflicts (e.g., over-subscription of resources) and resolves them individually by performing one or more plan modifications. CARACaS

CaS takes a most-committed, local, heuristic, iterative repair approach to producing and modifying plans. This approach gives CARACaS the advantages of (1) enabling the application of the repair algorithm, at any time, to any given plan at any level of abstraction or detail; (2) enabling rapid replanning when conditions or goals change; (3) facilitating incorporation of heuristics to prune the search space; and (4) incurring relatively low computational overhead during search inasmuch as a local repair algorithm does not require saving of intermediate plans or backtracking points.

*This work was done by Terrance Huntsberger, Hrand Aghazarian, Tara Estlin, and Daniel Gaines of Caltech for NASA's Jet Propulsion Laboratory. Further information is contained in a TSP (see page 1).*

*The software used in this innovation is available for commercial licensing. Please contact Karina Edmonds of the California Institute of Technology at (626) 395-2322. Refer to NPO-43635.*

## Algorithm for Wavefront Sensing Using an Extended Scene

The restriction to a point source has been removed.

NASA's Jet Propulsion Laboratory, Pasadena, California

A recently conceived algorithm for processing image data acquired by a Shack-Hartmann (SH) wavefront sensor is not subject to the restriction, previously applicable in SH wavefront sensing, that the image be formed from a distant star or other equivalent of a point light source. That is to say, the image could be of an extended scene. (One still has the option of using a point source.) The algorithm can be implemented in commercially available software on ordinary computers.

The steps of the algorithm are the following:

1. Suppose that the image comprises  $M$  sub-images. Determine the  $x,y$  Cartesian coordinates of the centers of these sub-images and store them in a  $2 \times M$  matrix.
2. Within each sub-image, choose an

$N \times N$ -pixel cell centered at the coordinates determined in step 1. For the  $l$ th sub-image, let this cell be denoted as  $s_l(x,y)$ . Let the cell of another sub-image (preferably near the center of the whole extended-scene image) be designated a reference cell, denoted  $r(x,y)$ .

3. Calculate the fast Fourier transforms of the sub-sub-images in the central  $N \times N$  portions (where  $N < N$  and both are preferably powers of 2) of  $r(x,y)$  and  $s_l(x,y)$ .
4. Multiply the two transforms to obtain a cross-correlation function  $C_l(u,v)$ , in the Fourier domain. Then let the phase of  $C_l(u,v)$  constitute a phase function,  $\phi(u,v)$ .
5. Fit  $u$  and  $v$  slopes to  $\phi(u,v)$  over a small  $u,v$  subdomain.
6. Compute the fast Fourier transform,  $S_l(u,v)$  of the full  $N \times N$  cell  $s_l(x,y)$ . Mul-

tiple this transform by the  $u$  and  $v$  phase slopes obtained in step 4. Then compute the inverse fast Fourier transform of the product.

7. Repeat steps 4 through 6 in an iteration loop, cumulating the  $u$  and  $v$  slopes, until a maximum iteration number is reached or the change in image shift becomes smaller than a predetermined tolerance.
8. Repeat steps 4 through 7 for the cells of all other sub-images.

This work was done by Erkin Sidick, Joseph Green, Catherine Ohara, and David Redding of Caltech for NASA's Jet Propulsion Laboratory. Further information is contained in a TSP (see page 1).

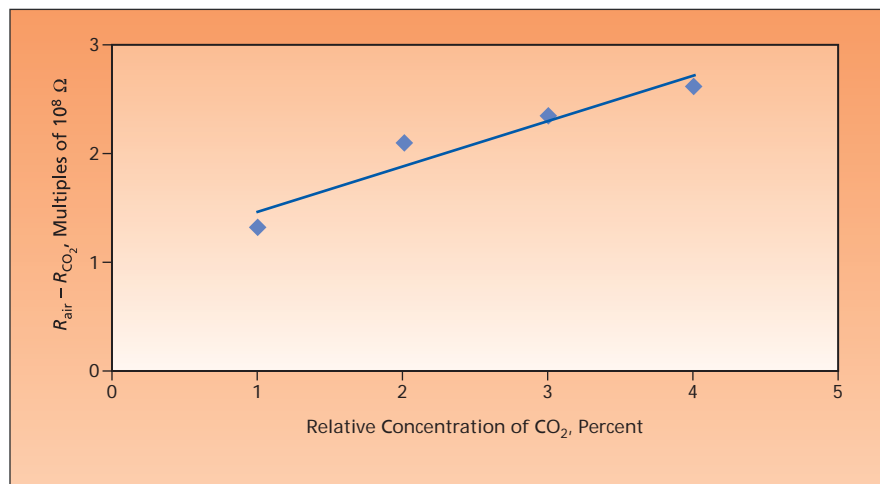
The software used in this innovation is available for commercial licensing. Please contact Karina Edmonds of the California Institute of Technology at (626) 395-2322. Refer to NPO-44770.

## CO<sub>2</sub> Sensors Based on Nanocrystalline SnO<sub>2</sub> Doped With CuO

Miniature CO<sub>2</sub> sensors could be mass-produced inexpensively.

John H. Glenn Research Center, Cleveland, Ohio

Nanocrystalline tin oxide (SnO<sub>2</sub>) doped with copper oxide (CuO) has been found to be useful as an electrical-resistance sensory material for measuring the concentration of carbon dioxide in air. SnO<sub>2</sub> is an n-type semiconductor that has been widely used as a sensing material for detecting such reducing gases as carbon monoxide, some of the nitrogen oxides, and hydrocarbons. Without doping, SnO<sub>2</sub> usually does not respond to carbon dioxide and other stable gases. The discovery that the electrical resistance of CuO-doped SnO<sub>2</sub> varies significantly with the concentration of CO<sub>2</sub> creates opportunities for the development of relatively inexpensive CO<sub>2</sub> sensors for detecting fires and monitoring atmospheric conditions. This discovery could also lead to research that could alter fundamental knowledge of SnO<sub>2</sub> as a sensing material, perhaps leading to the development of SnO<sub>2</sub>-based sensing materials for measuring concentrations of oxidizing gases.



The Electrical Resistance of a 1:8 CuO:SnO<sub>2</sub> film fabricated as described in the text was found to decrease as the concentration of CO<sub>2</sub> in air increased.  $R_{\text{air}}$  signifies the resistance of the film in pure air;  $R_{\text{CO}_2}$  signifies the resistance of the film at the indicated concentration of CO<sub>2</sub>.

Prototype CO<sub>2</sub> sensors based on CuO-doped SnO<sub>2</sub> have been fabricated by means of semiconductor-microfabrication and sol-gel nanomaterial-synthesis batch processes that are amendable to

inexpensive implementation in mass production. A fabrication process like that of the prototypes includes the following major steps:

1. Platinum interdigitated electrodes are

- microfabricated on a quartz substrate.
2. Nanocrystalline SnO<sub>2</sub> is synthesized in a partial sol-gel process. CuO dopant is synthesized through a precipitation process. The dopant and the sol-gel are mixed in proportions chosen to obtain the desired composition of the final product. One composition found to be suitable is a molar ratio of 1:8 CuO:SnO<sub>2</sub>.
  3. The dopant and sol-gel mixture is deposited in drops on (and across the gaps between) the electrodes.
  4. The workpiece is heated at a temperature of 700°C, converting the dopant

and sol-gel mixture to a film of nanocrystalline CuO doped SnO<sub>2</sub>.

In operation, a sensor of this type is heated to a temperature of 450°C while it is exposed to the CO<sub>2</sub> to be detected and the electrical resistance of the film between the electrodes is measured. Preliminary results of tests on a sensor containing a film of 1:8 CuO:SnO<sub>2</sub> showed an approximately linear response at CO<sub>2</sub> concentrations from 1 to 4 percent (see figure). In subsequent research and development efforts, it may be possible to increase sensitivities and/or reduce operating temperatures by combining

CuO-doped SnO<sub>2</sub> with solid-electrolyte materials.

*This work was done by Jennifer C. Xu and Gary W. Hunter of Glenn Research Center and Chung Chiu Liu and Benjamin J. Ward of Case Western Reserve University. Further information is contained in a TSP (see page 1).*

*Inquiries concerning rights for the commercial use of this invention should be addressed to NASA Glenn Research Center, Innovative Partnerships Office, Attn: Steve Fedor, Mail Stop 4-8, 21000 Brookpark Road, Cleveland, Ohio 44135. Refer to LEW-18247-1.*

## Improved Airborne System for Sensing Wildfires

**Unlike prior such systems, this system could be operated in daylight.**

*Stennis Space Center, Mississippi*

The Wildfire Airborne Sensing Program (WASP) is engaged in a continuing effort to develop an improved airborne instrumentation system for sensing wildfires. The system could also be used for other aerial-imaging applications, including mapping and military surveillance.

Unlike prior airborne fire-detection instrumentation systems, the WASP system would not be based on custom-made multispectral line scanners and associated custom-made complex optomechanical servomechanisms, sensors, readout circuitry, and packaging. Instead, the WASP system would be based on commercial off-the-shelf (COTS) equipment that would include (1) three or four electronic cameras (one for each of three or four wavelength bands) instead of a multispectral line scanner; (2) all associated drive and readout electronics; (3) a camera-pointing gimbal; (4) an inertial measurement unit (IMU) and a Global Positioning System (GPS) receiver for measuring the position, velocity, and orientation of the aircraft; and (5) a data-acquisition subsystem. It would be necessary to custom-develop an integrated sensor optical-bench assembly, a sensor-management subsystem, and software. The use of mostly COTS equipment is intended to reduce development time and cost, relative to those of prior systems.

The WASP system as envisioned (see figure) would include the three or four cameras, all aimed in the same direction, mounted in a camera subassembly. Three cameras would operate in the long-wavelength infrared (LWIR), medium-wavelength infrared (MWIR), and short-wavelength infrared (SWIR)

wavelength bands, respectively. The fourth camera, if included, would operate in the visible or visible plus near infrared (VNIR) wavelength band.

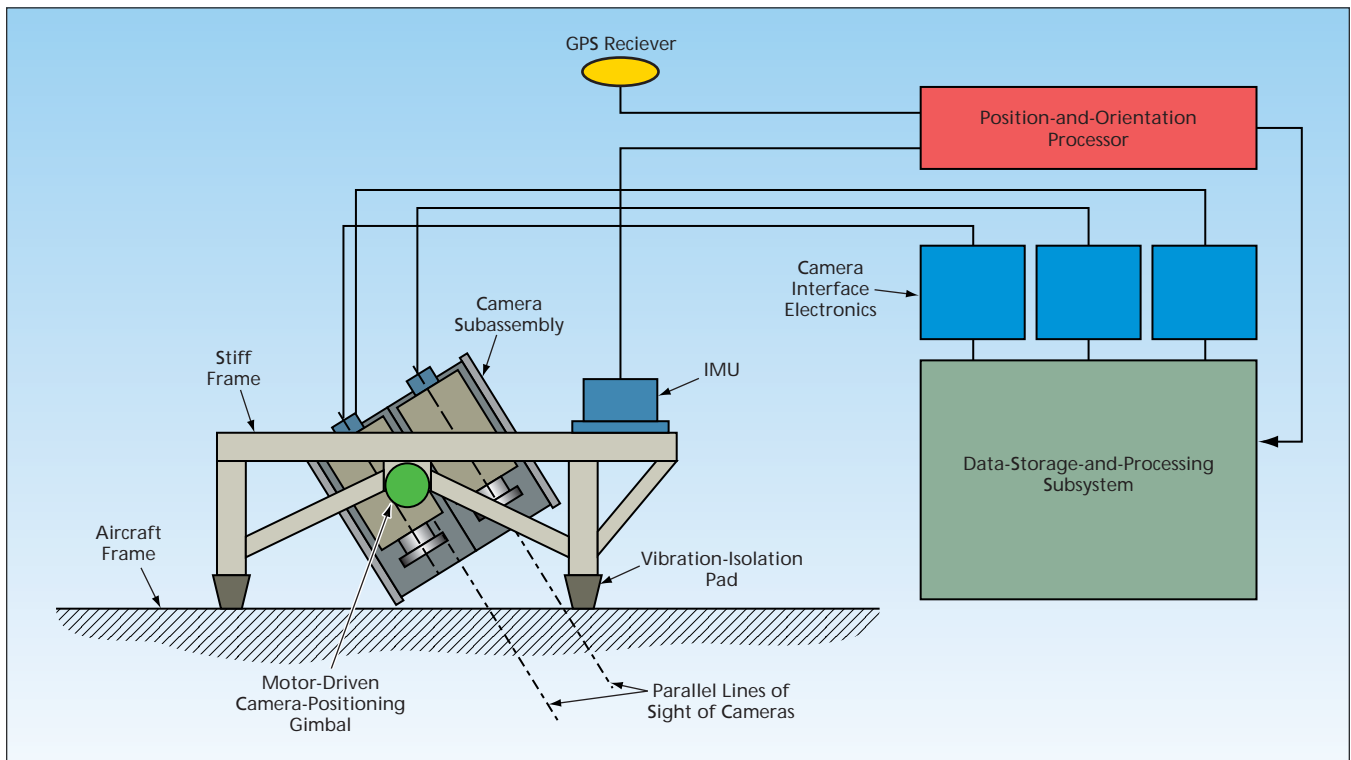
The camera subassembly would be mounted on the camera-positioning gimbal, which would scan the camera line of sight through a cross-track angular range of 40°. Because the half cone angle of the fields of view of the cameras would be 20°, this scanning action would provide coverage of a cross-track swath of 60°. Precise knowledge of the direction of the line of sight would be obtained from the combination of information provided by the GPS receiver, the inertial sensor subsystem, and a precise angle encoder mounted on the gimbal drive axis. Image data from the cameras and position and line-of-sight information would be sent to an on-board data-storage-and-processing subsystem. The estimated total weight of the system is less than 220 lb (equivalent to a mass <100 kg); the estimated maximum operating power of the system is <550 W.

In a typical fire-detection mission using a multispectral line-scanning instrumentation system, a 10-km-wide swath is imaged from an aircraft at an altitude of 3 km. Typically, missions are conducted at night to reduce false alarms attributable to solar heating. The MWIR band is used as the primary-fire detection band, along with an LWIR band, which provides scene context. A hot spot detected in the MWIR band can be located with respect to ground features imaged in the LWIR band. The line scanner provides excellent band-to-

band registration, but it is necessary to use a complex rate-controlled scanning mirror and significant post-processing to correct for variations between scan lines induced by variations in aircraft attitude and ground speed. The sensitive scanning mechanisms are also susceptible to failure and are difficult to service.

The WASP proposes to extend operation into the daytime and to improve operability. The extension into daytime would be enabled by the use of a SWIR camera in addition to the MWIR and LWIR cameras. (SWIR has been determined to be useful for discriminating fire targets in daylight and for detecting hot fires at night.) The fourth (visible or VNIR) camera, if included, would have very high resolution and would be used to provide detailed scene context during daylight operation.

In the WASP conceptual sequence of operation, the line of sight would be stepped across the swath between four discrete angular positions. The camera subassembly would be held steady at each angular position for a short time, during which the cameras would acquire image frames. The collection of frames would be assembled into a mosaic image spanning the cross-track swath. Because the frames would be acquired along momentarily steady lines of sight, there would be no need for complex rate-controlled servomechanisms. The motion of the aircraft would cause a small along-track offset between frames plus a small (typically, subpixel) smear during the image-integration (acquisition) time. Each of the four frames across the swath would be



The WASP System would include a gimbal that would aim several cameras operating in different spectral bands to acquire images at discrete angular increments to build a mosaic spectral image of a cross-track swath.

collected in at least three spectral bands (LWIR, MWIR, and SWIR at night or MWIR, SWIR, and visible or VNIR during the day), necessitating two registration steps. In the first step, the frames from the three spectral bands would be aligned into one frame. Then the frames

from the four angular positions would be aligned to produce the mosaic.

*This work was done by Donald McKeown and Michael Richardson of Rochester Institute of Technology for Stennis Space Center.*

*Inquiries concerning rights for its commercial use should be addressed to:*

*Rochester Institute of Technology  
54 Lomb Memorial Drive  
Rochester, NY 14623-5604  
E-mail: mckeown@cis.rit.edu*

*Refer to SSC-00241, volume and number of this NASA Tech Briefs issue, and the page number.*



## VHF Wide-Band, Dual-Polarization Microstrip-Patch Antenna

A dual-stacked-patch design incorporates several improvements over a basic design.

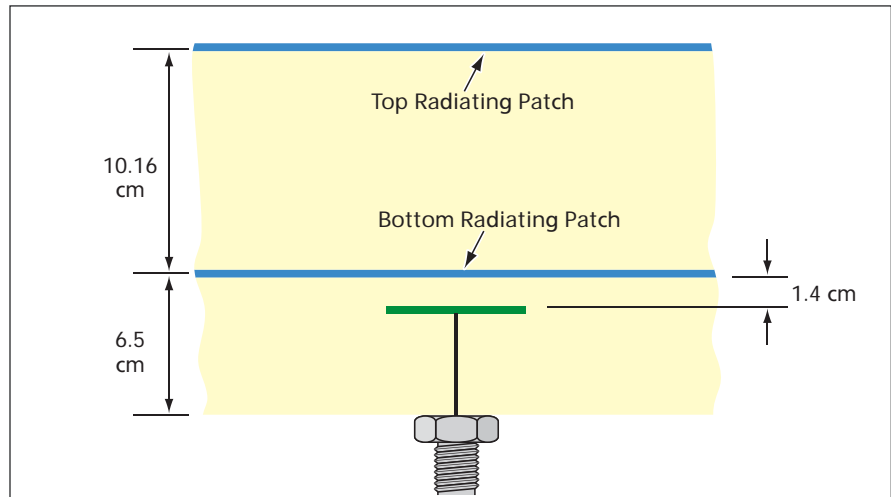
NASA's Jet Propulsion Laboratory, Pasadena, California

The figure depicts selected aspects of a very-high-frequency (VHF) microstrip-patch antenna designed and built to satisfy requirements specific to an airborne synthetic-aperture radar system for measuring the thickness of sea ice. One of the requirements is that the antenna be capable of functioning over the relatively wide frequency band of 127 to 172 MHz — corresponding to a fractional bandwidth of about 30 percent relative to a nominal mid-band frequency of 149.5 MHz. Another requirement is that the antenna be capable of functioning in either or both of two orthogonal linear polarizations. In addition, the antenna is required to be as compact and lightweight as possible.

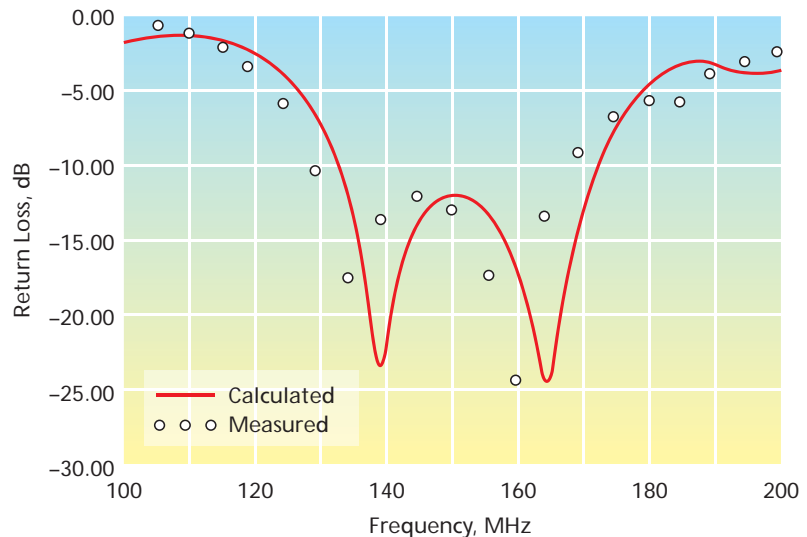
In a basic design according to generally accepted microstrip-patch-antenna-engineering practice, one would ordinarily use a relatively thick dielectric substrate and multiple feed probes to obtain the desired combination of wide-band and dual-polarization capabilities. However, the combination of a thick substrate and multiple feeds would give rise to higher-order electromagnetic nodes, thereby undesirably contributing to cross polarization and to reduction of the isolation between feed probes. To counter these adverse effects while satisfying the requirements stated above, the design of this antenna incorporates several improvements over the basic design.

The antenna features dual stacked square radiator patches, a ground plane, and relatively thick dielectric made of foam having a low value (1.05) of relative permittivity. The sides of the top and bottom radiator patches are 69.3 cm and 76.2 cm long, respectively. The patches are mechanically supported by the dielectric substrates. The bottom radiator patch lies 6.5 cm above the ground plane, which is a square of side length 117 cm. The top radiator patch lies 10.16 cm above the bottom radiator patch.

The bottom radiator patch is excited via square capacitive feed probes, the capacitive patches of which have a side length of 6.35 cm. The top radiator



PARTLY SCHEMATIC CROSS SECTION OF PORTION CONTAINING A FEED PROBE



MEASURED AND CALCULATED INPUT RETURN LOSS

This Dual-Polarization Microstrip-Patch Antenna incorporates several design features to enable wide-band operation with minimal cross polarization and minimal coupling between orthogonal pairs of feed probes.

patch is excited parasitically from the bottom radiator patch. Four feed probes (instead of the minimum of two feed probes needed for dual polarization) are used to increase the wide-band capability, suppress higher-order

modes, and reduce cross-polarization levels. Each probe is located 2.54 cm from the center of the antenna and its capacitive patch is located 1.4 cm below the bottom radiator patch. Within each pair of oppositely located

feed probes, the two probes are excited 180° out of phase with each other to suppress higher-order modes. For additional suppression of higher-order modes, a shorting pin is soldered to both the upper and lower patches and the ground plane at the center of the antenna.

In the absence of corrective action, the use of four feed probes and thick substrates would result in unacceptably large amounts of coupling between oppositely located probes. To reduce this coupling, 24 additional shorting pins, located along the two axes of symmetry, are soldered between the bottom patch and the ground

plane. Power is coupled to the antenna via two 180° hybrids, each for exciting one of the pairs of oppositely located probes.

*This work was done by John Huang of Caltech for NASA's Jet Propulsion Laboratory. For further information, contact iaoffice@jpl.nasa.gov. NPO-41502*

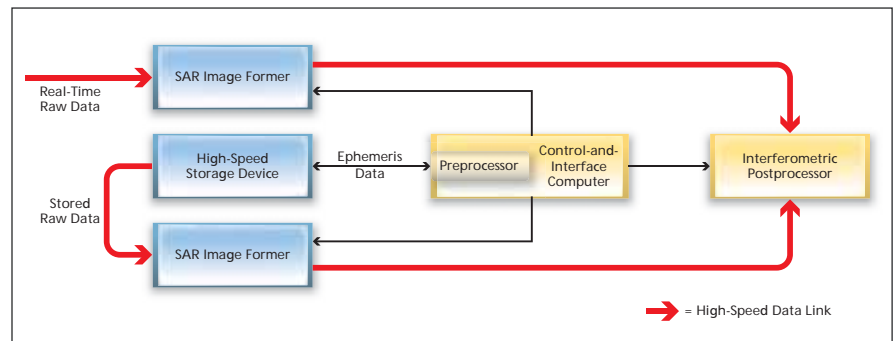
## Onboard Data Processor for Change-Detection Radar Imaging

This system could be used to map earthquakes, landslides, floods, and wildfires.

NASA's Jet Propulsion Laboratory, Pasadena, California

A computer system denoted a change-detection onboard processor (CDOP) is being developed as a means of processing the digitized output of a synthetic-aperture radar (SAR) apparatus aboard an aircraft or spacecraft to generate images showing changes that have occurred in the terrain below between repeat passes of the aircraft or spacecraft over the terrain. When fully developed, the CDOP is intended to be capable of generating SAR images and/or SAR differential interferograms in nearly real time. The CDOP is expected to be especially useful for understanding some large-scale natural phenomena and/or mitigating natural hazards: For example, it could be used for near-real-time observation of surface changes caused by floods, landslides, forest fires, volcanic eruptions, earthquakes, glaciers, and sea ice movements. It could also be used to observe such longer-term surface changes as those associated with growth of vegetation (relevant to estimation of wild-fire fuel loads).

The CDOP is, essentially, an interferometric SAR processor designed to operate aboard a radar platform. The CDOP design features a compact processor architecture chosen to combine the flexibility of microprocessors with the very high speed of field-programmable gate arrays (FPGAs) so as to optimize throughput performance while maintaining flexibility. The processor design addresses three critical requirements of real-time, onboard processing hardware for interferometric SAR imaging: high computational throughput, a large amount of onboard memory, and high-speed data interconnections throughout the processing chain. The functional blocks of the CDOP (see figure) include the following:



Real-Time and Stored Raw Radar Data are processed in the CDOP to generate images of surface changes in scanned terrain.

- **Preprocessor** — A microprocessor within a control-and-interface computer serves as a preprocessor that generates parameters necessary for generation of SAR image data from a combination of ephemeris and radar-configuration data. For the ephemeris data, the preprocessor implements a six-state (three position and three velocity coordinates) Kalman filter to effect real-time reconstruction of the platform trajectory from the outputs of an inertial navigation unit and a Global Positioning System receiver. The preprocessor also includes an azimuth pre-summer to decimate and re-align range-compressed data in the along-track direction, and an optional motion compensation-module for airborne interferometric SAR. The output of the preprocessor is utilized by the SAR image formers described next.
- **SAR Image Formers** — The raw SAR data are processed into SAR image data by two FPGA SAR processors that implement a range-Doppler algorithm with motion-compensation capability. The two SAR processors accept two input streams of raw radar data: typically, these would be (1) the real-time stream of data from the high-speed

digital back end of the operating radar apparatus and (2) a stream of corresponding data from a previous pass retrieved from a high-speed storage device via a fiber-optic link. Alternatively, if the radar platform were to include two radar apparatuses in an interferometric configuration, then the CDOP could process the near-real-time streams of data from these apparatuses for use in generating a single-pass interferogram.

- **Interferometric Postprocessor** — Another microprocessor generates SAR interferometric image data from the outputs of the two SAR processors. In a typical application, the output of this processor would be transmitted to a ground station (downlinked). Because all of the processing up to the point of downlinking would be done onboard, the downlink data rate necessary for observing changes in the terrain would be significantly reduced.

*This work was done by Yunling Lou, Ronald J. Muellerschoen, Steve A. Chien, and Sasan S. Saatchi Caltech and Duane Clark of Leeward Engineering for NASA's Jet Propulsion Laboratory. Further information is contained in a TSP (see page 1). NPO-45751*

# Using LDPC Code Constraints To Aid Recovery of Symbol Timing

Performance would approach within  $\approx 0.2$  dB of that of perfect timing.

NASA's Jet Propulsion Laboratory, Pasadena, California

A method of utilizing information available in the constraints imposed by a low-density parity-check (LDPC) code has been proposed as a means of aiding the recovery of symbol timing in the reception of a binary-phase-shift-keying (BPSK) signal representing such a code in the presence of noise, timing error, and/or Doppler shift between the transmitter and the receiver. This method and the receiver architecture in which it would be implemented belong to a class of timing-recovery methods and corresponding receiver architectures characterized as pilotless in that they do not require transmission and reception of pilot signals.

Acquisition and tracking of a signal of the type described above have traditionally been performed upstream of, and independently of, decoding and have typically involved utilization of a phase-locked loop (PLL). However, the LDPC decoding process, which is iterative, provides information that can be fed back to the timing-recovery receiver circuits to improve performance significantly over that attainable in the absence of such feedback. Prior methods of coupling LDPC decoding with timing recovery had focused on the use of output code words produced as the iterations progress. In contrast, in the present method, one exploits the information available from the metrics computed for the constraint nodes of an LDPC code during the decoding process. In addition, the method involves the use of a waveform model that captures, better than do the waveform models of the

prior methods, distortions introduced by receiver timing errors and transmitter/receiver motions.

An LDPC code is commonly represented by use of a bipartite graph containing two sets of nodes. In the graph corresponding to an  $(n, k)$  code, the  $n$  variable nodes correspond to the code word symbols and the  $n-k$  constraint nodes represent the constraints that the code places on the variable nodes in order for them to form a valid code word. The decoding procedure involves iterative computation of values associated with these nodes. A constraint node represents a parity-check equation using a set of variable nodes as inputs. A valid decoded code word is obtained if all parity-check equations are satisfied. After each iteration, the metrics associated with each constraint node can be evaluated to determine the status of the associated parity check. Heretofore, normally, these metrics would be utilized only within the LDPC decoding process to assess whether or not variable nodes had converged to a codeword. In the present method, it is recognized that these metrics can be used to determine accuracy of the timing estimates used in acquiring the sampled data that constitute the input to the LDPC decoder. In fact, the number of constraints that are 'satisfied' exhibits a peak near the optimal timing estimate. Coarse timing estimation (or first-stage estimation as described below) is found via a parametric search for this peak.

The present method calls for a two-stage receiver architecture illustrated in the figure. The first stage would correct

large time delays and frequency offsets; the second stage would track random walks and correct residual time and frequency offsets. In the first stage, constraint-node feedback from the LDPC decoder would be employed in a search algorithm in which the searches would be performed in successively narrower windows to find the correct time delay and/or frequency offset. The second stage would include a conventional first-order PLL with a decision-aided timing-error detector that would utilize, as its decision aid, decoded symbols from the LDPC decoder.

The method has been tested by means of computational simulations in cases involving various timing and frequency errors. The results of the simulations in the ideal case of perfect timing in the receiver.

*This work was done by Christopher Jones, John Villasnor, Dong-U Lee, and Esteban Valles of Caltech for NASA's Jet Propulsion Laboratory.*

*In accordance with Public Law 96-517, the contractor has elected to retain title to this invention. Inquiries concerning rights for its commercial use should be addressed to:*

*Innovative Technology Assets Management  
JPL*

*Mail Stop 202-233*

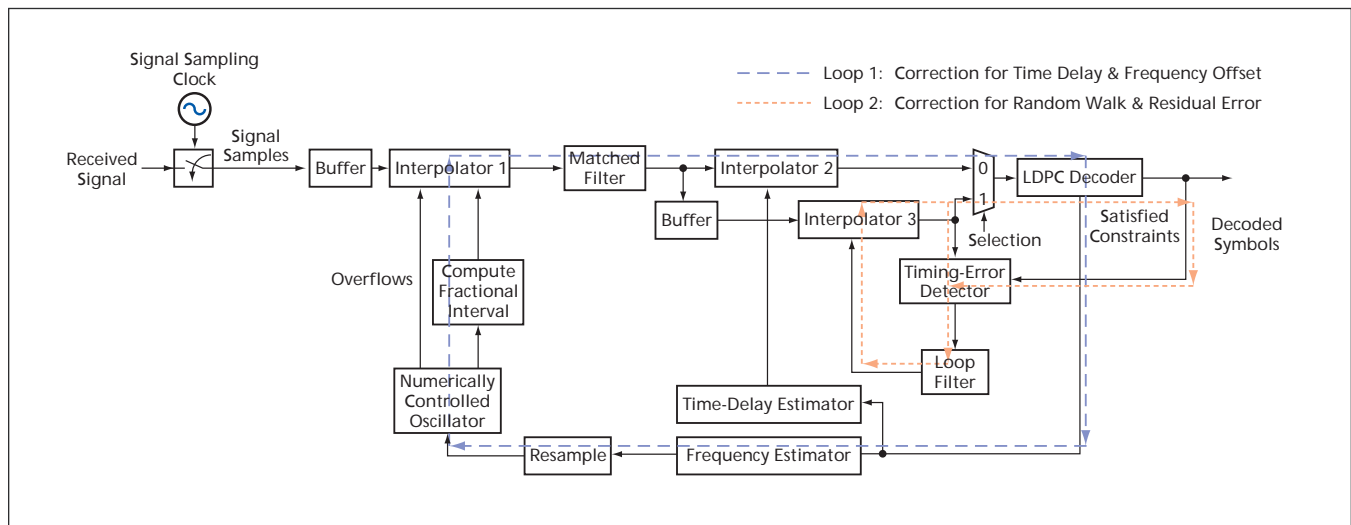
*4800 Oak Grove Drive*

*Pasadena, CA 91109-8099*

*(818) 354-2240*

*E-mail: iaoffice@jpl.nasa.gov*

*Refer to NPO-43112, volume and number of this NASA Tech Briefs issue, and the page number.*



Two Stages of Timing Recovery would be effected by corresponding two signal-processing loops.

---

## System for Measuring Flexing of a Large Spaceborne Structure

*NASA's Jet Propulsion Laboratory, Pasadena, California*

An optoelectronic metrology system is used for determining the attitude and flexing of a large spaceborne radar antenna or similar structure. The measurements are needed for accurate pointing of the antenna and correction and control of the phase of the radar signal wavefront. The system includes a dual-field-of-view star tracker; a laser ranging unit (LRU) and a position-sensitive-detector (PSD)-based camera mounted on an optical bench; and fidu-

cial targets at various locations on the structure.

The fiducial targets are illuminated in sequence by laser light coupled via optical fibers. The LRU and the PSD provide measurements of the position of each fiducial target in a reference frame attached to the optical bench. During routine operation, the star tracker utilizes one field of view and functions conventionally to determine the orientation of the optical bench. During operation in a calibration mode, the star

tracker also utilizes its second field of view, which includes stars that are imaged alongside some of the fiducial targets in the PSD; in this mode, the PSD measurements are traceable to star measurements.

*This work was done by Carl Christian Liebe, Alexander Abramovici, Randy Bartman, Keith Coste, Edward Litty, Jacob Chapsky, Raymond Lam, Sergei Jerebets, John Schmalz, and Lars Chapsky of Caltech for NASA's Jet Propulsion Laboratory. For more information, contact iaoffice@jpl.nasa.gov. NPO-45076*

---

## Integrated Formation Optical Communication and Estimation System

**Formation estimation couples estimation algorithms, sensing topology, and communication topology.**

*NASA's Jet Propulsion Laboratory, Pasadena, California*

An architecture has been designed that integrates formation estimation methodologies, precision formation sensing, and high-bandwidth formation communication into a robust, strap-on system that meets knowledge and communication requirements for the majority of planned, precision formation missions. Specifically, the integrated system supports (a) sub-millimeter metrology, (b) multiple >10 Mbps communication channels over a large, 10° field-of-view (FOV), and (c) generalized formation estimation methodologies. The sensing sub-system consists of several absolute, metrology gauges with up to 0.1 mm precision that use amplitude-modulated lasers and a LISA-heritage phase meter. Since amplitude modulation is used, inexpensive and robust diode lasers may be used instead of complex, frequency-stabilized lasers such as for nanometer-level metrology. The metrology subsystem laser transceivers consist of a laser diode, collecting optics, and an ava-

lanche photo diode (APD) for detecting incoming laser signals. The APD is necessary since received power is small due to the large (for optical applications) FOV. The phase meter determines the phase of the incoming amplitude modulations as measured by the APD. This phase is equivalent to time-of-flight and, therefore, distance.

By placing three laser transceivers on each spacecraft, 18 clock-offset-corruped distances are calculated. These measurements are communicated and averaged to obtain nine correct distances between the transceivers. From these correct distances, the range and bearing between spacecraft and their relative attitude are determined.

Next, communication is integrated on the laser carrier through spectral separation. Metrology amplitude modulations are limited to the 45–50 MHz band, leaving 0–45 MHz for communication. Through careful design of coding scheme, error correction, and filters, six

independent 10 Mbps receive channels are possible. Hence, a spacecraft can simultaneously broadcast at 10 Mbps and listen to six other spacecraft.

The integrated sensing and communication architecture has been developed, as have formation estimation methodologies that allow the sensing topology to reconfigure as spacecraft maneuver. A bench-top implementation of the integrated sensing and communication architecture is in progress. The final, multiple sensing/communication systems will be tied together via formation estimation algorithms that are also undergoing further development.

*This work was done by Daniel Scharf, Andreas Kuhnert, Joseph Kovalik, Fred Hadaegh, and Daniel Shaddock of Caltech for NASA's Jet Propulsion Laboratory.*

*The software used in this innovation is available for commercial licensing. Please contact Karina Edmonds of the California Institute of Technology at (626) 395-2322. Refer to NPO-44558.*



## **☐ Making Superconducting Welds Between Superconducting Wires**

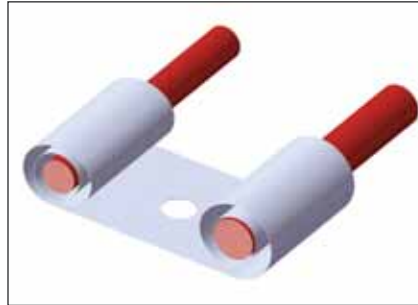
**Parts of a superconducting circuit can be made from different metals.**

*NASA's Jet Propulsion Laboratory, Pasadena, California*

A technique for making superconducting joints between wires made of dissimilar superconducting metals has been devised. The technique is especially suitable for fabrication of superconducting circuits needed to support persistent electric currents in electromagnets in diverse cryogenic applications. Examples of such electromagnets include those in nuclear magnetic resonance (NMR) and magnetic resonance imaging (MRI) systems and in superconducting quantum interference devices (SQUIDS).

Sometimes, it is desirable to fabricate different parts of a persistent-current-supporting superconducting loop from different metals. For example, a sensory coil in a SQUID might be made of Pb, a Pb/Sn alloy, or a Cu wire plated with Pb/Sn, while the connections to the sensory coil might be made via Nb or Nb/Ti wires. Conventional wire-bonding techniques, including resistance spot welding and pressed contact, are not workable because of large differences between the hardnesses and melting

temperatures of the different metals. The present technique is not subject to this limitation.



One or More Wire(s) can be spark-welded to the inside of a tube made by rolling a piece of Nb foil.

The present technique involves the use (1) of a cheap, miniature, easy-to-operate, capacitor-discharging welding apparatus that has an Nb or Nb/Ti tip and operates with a continuous local flow of gaseous helium and (2) preparation of a joint in a special spark-discharge welding geometry. In a typical application, a piece of Nb foil about 25  $\mu\text{m}$  thick is rolled to form a tube, into which

is inserted a wire that one seeks to weld to the tube (see figure). The tube can be slightly crimped for mechanical stability. Then a spark weld is made by use of the aforementioned apparatus with energy and time settings chosen to melt a small section of the niobium foil. The energy setting corresponds to the setting of a voltage to which the capacitor is charged.

In an experiment, the technique was used to weld an Nb foil to a copper wire coated with a Pb/Sn soft solder, which is superconducting. The joint was evaluated as part of a persistent-current circuit having an inductance of 1 mH. A current was induced in a loop, and no attenuation of the current after a time interval 1,000 s was discernible in a measurement having a fractional accuracy of  $10^{-4}$ . This observation supports the conclusion that the weld had an electrical resistance  $<10^{-10} \Omega$ .

*This work was done by Konstantin I. Penanen, Inseob Hahn, and Byeong Ho Eom of Caltech for NASA's Jet Propulsion Laboratory. Further information is contained in a TSP (see page 1). NPO-45931*

## **☐ Method for Thermal Spraying of Coatings Using Resonant-Pulsed Combustion**

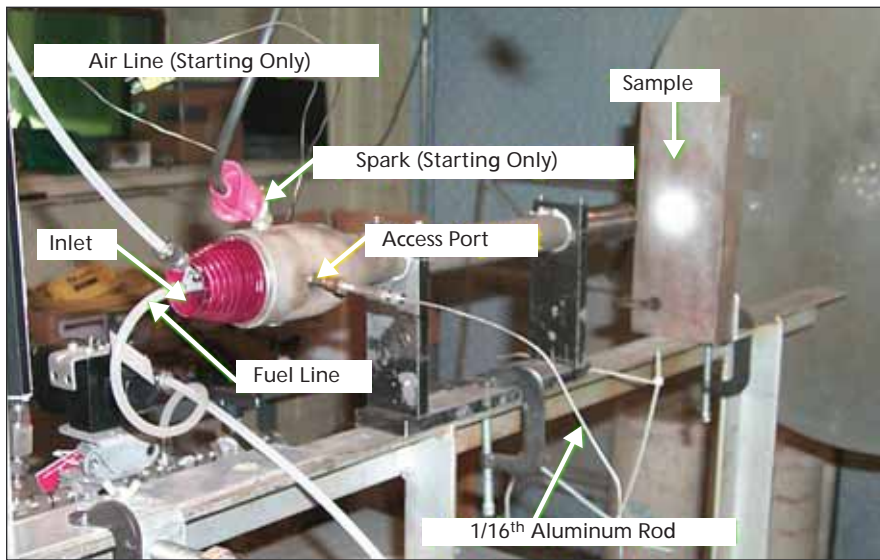
**High-volume, high-velocity surface deposition allows protective metal coatings to be applied to otherwise vulnerable surfaces.**

*John H. Glenn Research Center, Cleveland, Ohio*

A method has been devised for high-volume, high-velocity surface deposition of protective metallic coatings on otherwise vulnerable surfaces. Thermal spraying is used whereby the material to be deposited is heated to the melting point by passing through a flame. Rather than the usual method of deposition from the jet formed from the combustion products, this innovation uses non-steady combustion (i.e. high-frequency, periodic, confined bursts), which generates not only higher temperatures and heat transfer rates, but exceedingly high im-

pingement velocities an order of magnitude higher than conventional thermal systems. Higher impingement rates make for better adhesion. The high heat transfer rates developed here allow the deposition material to be introduced, not as an expensive powder with high surface-area-to-volume, but in convenient rod form, which is also easier and simpler to feed into the system. The nonsteady, resonant combustion process is self-aspirating and requires no external actuation or control and no high-pressure supply of fuel or air.

The innovation has been demonstrated using a commercially available resonant combustor shown in the figure. Fuel is naturally aspirated from the tank through the lower Tygon tube and into the pulsejet. Air for starting is ported through the upper Tygon tube line. Once operation commences, this air is no longer needed as additional air is naturally aspirated through the inlet. A spark plug on the device is needed for starting, but the process carries on automatically as the operational device is resonant and reignites itself with each 220-Hz pulse.



A Reproduction of the Pulsejet is shown mounted on a test stand. Flow is from left to right.

Through a small access port in the side of the device, the aluminum rod material is deposited into the combustion chamber. Thrust production from the combus-

tor results creates a periodic, high-speed jet, which is emitted from the tailpipe, downstream of the combustion chamber. The material to be deposited melts in the

combustion chamber, and then is carried downstream and ejected from the tailpipe at high speed where it impinges and solidifies on the target surface. The residence times in the combustion chamber for the material to be deposited are low. By avoiding overheating, problems like further chemical changes (like oxidation) are avoided.

This sort of device is mechanically simple and has potential to be used to create a mobile, high-volume spray unit. The only external power required would be needed to control and actuate the feeding of the coating material into the device.

*This work was done by Daniel E. Paxson of Glenn Research Center. Further information is contained in a TSP (see page 1).*

*Inquiries concerning rights for the commercial use of this invention should be addressed to NASA Glenn Research Center, Innovative Partnerships Office, Attn: Steve Fedor, Mail Stop 4-8, 21000 Brookpark Road, Cleveland, Ohio 44135. Refer to LEW-18221-1.*



## Coating Reduces Ice Adhesion

Developed for the space shuttle, this coating may be used on aircraft and automobiles.

*John F. Kennedy Space Center, Florida*

The Shuttle Ice Liberation Coating (SILC) has been developed to reduce the adhesion of ice to surfaces on the space shuttle. SILC, when coated on a surface (foam, metal, epoxy primer, polymer surfaces), will reduce the adhesion of ice by as much as 90 percent as compared to the corresponding uncoated surface. This innovation is a durable coating that can withstand several cycles of ice growth and removal without loss of anti-adhesion properties.

SILC is made of a binder composed of varying weight percents of siloxane(s), ethyl alcohol, ethyl sulfate, isopropyl alcohol, and of fine-particle polytetrafluoroethylene (PTFE). The combination of these components produces a coating

with significantly improved weathering characteristics over the siloxane system alone.

In some cases, the coating will delay ice formation and can reduce the amount of ice formed. SILC is not an ice prevention coating, but the very high water contact angle (greater than 140°) causes water to readily run off the surface. This coating was designed for use at temperatures near -170 °F (-112 °C). Ice adhesion tests performed at temperatures from -170 to 20 °F (-112 to -7 °C) show that SILC is a very effective ice release coating.

SILC can be left as applied (opaque) or buffed off until the surface appears clear. Energy dispersive spectroscopy

(EDS) and x-ray photoelectron spectroscopy (XPS) data show that the coating is still present after buffing to transparency. This means SILC can be used to prevent ice adhesion even when coating windows or other objects, or items that require transmission of optical light. Car windshields are kept cleaner and SILC effectively mitigates rain and snow under driving conditions.

*This work was done by Trent Smith of Kennedy Space Center; Michael Prince, Charles DeWeese and Leslie Curtis of Marshall Space Flight Center; and Erik Weiser and Roberto Cano of Langley Research Center. For more information, contact the Kennedy Space Center Innovative Partnership Program Office at (321) 861-7158. KSC-13100/1.*

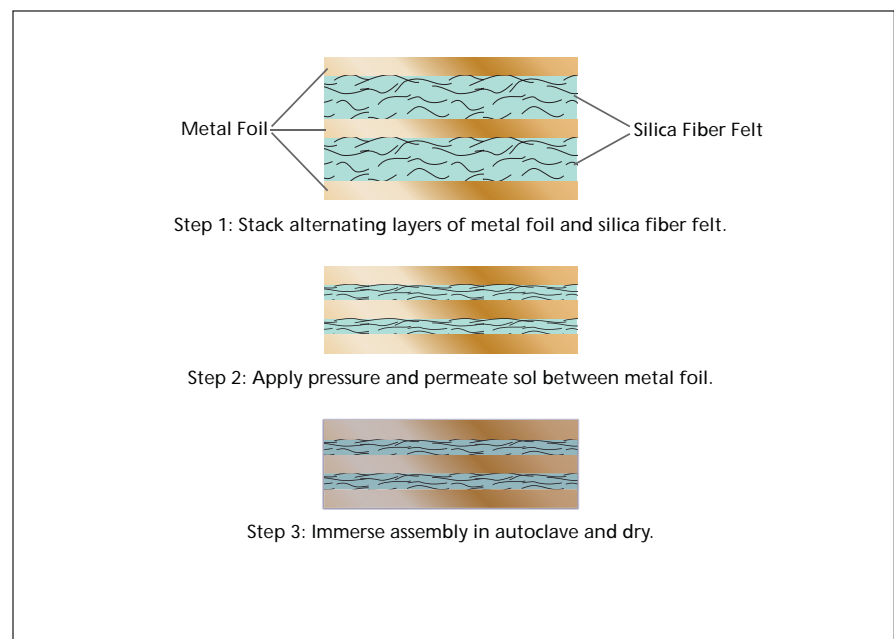
## Hybrid Multifoil Aerogel Thermal Insulation

Aerogel used in place of astroquartz makes lighter, more efficient insulation.

*NASA's Jet Propulsion Laboratory, Pasadena, California*

This innovation blends the merits of multifoil insulation (MFI) with aerogel-based insulation to develop a highly versatile, ultra-low thermally conductive material called hybrid multifoil aerogel thermal insulation (HyMATI). The density of the opacified aerogel is 240 mg/cm<sup>3</sup> and has thermal conductivity in the 20 mW/mK range in high vacuum and 25 mW/mK in 1 atmosphere of gas (such as argon) up to 800 °C. It is stable up to 1,000 °C. This is equal to commercially available high-temperature thermal insulation. The thermal conductivity of the aerogel is 36 percent lower compared to several commercially available insulations when tested in 1 atmosphere of argon gas up to 800 °C.

Layers of metal foil block infrared radiation (IR), which are separated by thin (100–1,000-micron) layers of opacified aerogel (see figure). The aerogel further reduces IR transport and, more importantly, significantly reduces gas and solid conduction when compared to the astroquartz used in heritage MFI (that used



HyMATI Blends Multiple Layers of Foil Separated by Fiber Reinforced, Opacified Aerogel. Fabrication consists of: (a) stacking alternating layers of reflective metal foil and high purity quartz fiber, (b) applying slight pressure to the stack to control the spacing between metal foil layers, and (c) permeating the liquid aerogel precursor into the stack, followed by solidification and supercritical drying.

7.6-micron thick molybdenum foil separated by  $\approx$ 90-micron thick astroquartz with 60 layers of each forming a stack 1.7 cm thick). By replacing the astroquartz with JPL-developed aerogel, the overall mass of MFI is reduced by 36 percent. Further reductions in mass may also be had by selecting lower density metal foils, such as titanium, zirconium, or reflective Grafoil<sup>®</sup>. In addition to mass reduction benefits, HyMATI is a tunable insulation that can be tailored for use in various temperature ranges up to 1,000 °C, and can be considered for use in space vacuum,

with a cover gas such as argon or xenon or on other planets with atmosphere.

By replacing heritage MFI with aerogel, the HyMATI will reduce the mass of future RPS (radioisotope power systems) technology. Also, the aerogel has the lowest gas conductivity of any material in its class, enabling RPS operation in vacuum, cover gas, or atmosphere. This means enabling a single RPS design for all NASA missions requiring RPS as opposed to current situations where NASA has a Multi-Mission RTG (for Mars Science Laboratory, for example) and

GPHS-RTG (General-Purpose Heat Source-Radioisotope Thermoelectric Generator) for deep-space exploration.

*This work was done by Jeffrey Sakamoto, Jong-Ah Paik, Steven Jones, and Bill Nesmith of Caltech for NASA's Jet Propulsion Laboratory. Further information is contained in a TSP (see page 1).*

*This invention is owned by NASA, and a patent application has been filed. Inquiries concerning nonexclusive or exclusive license for its commercial development should be addressed to the Patent Counsel, NASA Management Office-JPL. Refer to NPO-45219.*



## SHINE Virtual Machine Model for In-flight Updates of Critical Mission Software

This software is a new target for the Spacecraft Health Inference Engine (SHINE) knowledge base that compiles a knowledge base to a language called Tiny C — an interpreted version of C that can be embedded on flight processors. This new target allows portions of a running SHINE knowledge base to be updated on a “live” system without needing to halt and restart the containing SHINE application. This enhancement will directly provide this capability without the risk of software validation problems and can also enable complete integration of BEAM and SHINE into a single application.

This innovation enables SHINE deployment in domains where autonomy is used during flight-critical applications that require updates. This capability eliminates the need for halting the application and performing potentially serious total system uploads before resuming the application with the loss of system integrity. This software enables additional applications at JPL (microsensors, embedded mission hardware) and increases the marketability of these applications outside of JPL.

*This work was done by Mark James, Ryan Mackey, and Raffi Tikidjian of Caltech for NASA's Jet Propulsion Laboratory. Further information is contained in a TSP (see page 1).*

*In accordance with Public Law 96-517, the contractor has elected to retain title to this invention. Inquiries concerning rights for its commercial use should be addressed to:*

*Innovative Technology Assets Management  
JPL  
Mail Stop 202-233  
4800 Oak Grove Drive  
Pasadena, CA 91109-8099  
E-mail: iaoffice@jpl.nasa.gov  
Refer to NPO-44547, volume and number of this NASA Tech Briefs issue, and the page number.*

## Mars Image Collection Mosaic Builder

A computer program assembles images from the Mars Global Surveyor (MGS) Mars Observer Camera Narrow Angle (MOCNA) collection to generate a uniform-high-resolution, georefer-

enced, uncontrolled mosaic image of the Martian surface. At the time of reporting the information for this article, the mosaic covered 7 percent of the Martian surface and contained data from more than 50,000 source images acquired under various light conditions at various resolutions.

The program geolocates, reprojects, and blends one source image at a time onto the mosaic. Geolocation and reprojection involve the use of a second-order polynomial based on coordinates of the source-image footprints. Images are stacked in the order of increasing resolution — higher-resolution images on top of lower-resolution images. The stacking order is also partly determined by the order of adding the source images to the mosaic. The mosaic-image data are stored in a custom file format that accommodates regional tiles and supports explicit representation of empty areas, image-data compression, and representation of localized changes.

The program is written as a script in the ImageTCL software of Silicon Graphics, Inc. (SGI), using SGI Image Vision Library with extensions specific to a geographic information system.

*This program was written by Lucian Plesea of Caltech and Trent Hare of the United States Geological Survey for NASA's Jet Propulsion Laboratory.*

*This software is available for commercial licensing. Please contact Karina Edmonds of the California Institute of Technology at (626) 395-2322. Refer to NPO-45960.*

## Providing Internet Access to High-Resolution Mars Images

The OnMars server is a computer program that provides Internet access to high-resolution Mars images, maps, and elevation data, all suitable for use in geographical information system (GIS) software for generating images, maps, and computational models of Mars. The OnMars server is an implementation of the Open Geospatial Consortium (OGC) Web Map Service (WMS) server. Unlike other Mars Internet map servers that provide Martian data using an Earth coordinate system, the OnMars WMS server supports encoding of data in Mars-specific coordinate systems.

The OnMars server offers access to most of the available high-resolution Martian image and elevation data, including an 8-meter-per-pixel uncontrolled mosaic of most of the Mars Global Surveyor (MGS) Mars Observer Camera Narrow Angle (MOCNA) image collection, which is not available elsewhere. This server can generate image and map files in the tagged image file format (TIFF), Joint Photographic Experts Group (JPEG), 8- or 16-bit Portable Network Graphics (PNG), or Keyhole Markup Language (KML) format. Image control is provided by use of the OGC Style Layer Descriptor (SLD) protocol. The OnMars server also implements tiled WMS protocol and superoverlay KML for high-performance client application programs.

*This program was written by Lucian Plesea of Caltech and Trent Hare of the United States Geological Survey for NASA's Jet Propulsion Laboratory.*

*This software is available for commercial licensing. Please contact Karina Edmonds of the California Institute of Technology at (626) 395-2322. Refer to NPO-45959.*

## Providing Internet Access to High-Resolution Lunar Images

The OnMoon server is a computer program that provides Internet access to high-resolution Lunar images, maps, and elevation data, all suitable for use in geographical information system (GIS) software for generating images, maps, and computational models of the Moon. The OnMoon server implements the Open Geospatial Consortium (OGC) Web Map Service (WMS) server protocol and supports Moon-specific extensions. Unlike other Internet map servers that provide Lunar data using an Earth coordinate system, the OnMoon server supports encoding of data in Moon-specific coordinate systems.

The OnMoon server offers access to most of the available high-resolution Lunar image and elevation data. This server can generate image and map files in the tagged image file format (TIFF) or the Joint Photographic Experts Group (JPEG), 8- or 16-bit Portable Network Graphics (PNG), or Keyhole Markup Language (KML) format. Image control is provided

by use of the OGC Style Layer Descriptor (SLD) protocol. Full-precision spectral arithmetic processing is also available, by use of a custom SLD extension. This server can dynamically add shaded relief based on the Lunar elevation to any image layer. This server also implements tiled WMS protocol and super-overlay KML for high-performance client application programs.

*This program was written by Lucian Plesea of Caltech and Trent Hare of the United States Geological Survey for NASA's Jet Propulsion Laboratory.*

*This software is available for commercial licensing. Please contact Karina Edmonds of the California Institute of Technology at (626) 395-2322. Refer to NPO-45951.*

---

### Expressions Module for the Satellite Orbit Analysis Program

The Expressions Module is a software module that has been incorporated into the Satellite Orbit Analysis Program (SOAP). The module includes an expressions-parser submodule built on top of an analytical system, enabling the user to define logical and numerical variables and constants. The variables can capture output from SOAP orbital-prediction and geometric-engine computations. The module can combine variables and constants with built-in logical operators (such as Boolean AND, OR, and NOT), relational operators (such as  $>$ ,  $<$ , or  $=$ ), and mathematical operators (such as addition, subtraction, multiplication, division, modulus, exponentiation, differentiation, and integration). Parentheses can be used to specify precedence of operations.

The module contains a library of mathematical functions and operations, including logarithms, trigonometric functions, Bessel functions, minimum/maximum operations, and floating-point-to-integer conversions. The module supports combinations of time, distance, and angular units and has a dimensional-analysis component that checks for correct usage of units. A parser based on the Flex language and the Bison program looks for and indicates errors in syntax. SOAP expressions can be built using other expressions as arguments, thus enabling the user to build analytical trees. A graphical user interface facilitates use.

*This program was developed by Robert Carnright, David Stodden, Jim Paget, and John Coggi of Caltech for NASA's Jet Propulsion Laboratory.*

*This software is available for commercial licensing. Please contact Karina Edmonds of the California Institute of Technology at (626) 395-2322. Refer to NPO-45052.*

---

### Virtual Satellite

Virtual Satellite (VirtualSat) is a computer program that creates an environment that facilitates the development, verification, and validation of flight software for a single spacecraft or for multiple spacecraft flying in formation. In this environment, enhanced functionality and autonomy of navigation, guidance, and control systems of a spacecraft are provided by a virtual satellite — that is, a computational model that simulates the dynamic behavior of the spacecraft.

Within this environment, it is possible to execute any associated software, the development of which could benefit from knowledge of, and possible interaction (typically, exchange of data) with, the virtual satellite. Examples of associated software include programs for simulating spacecraft power and thermal-management systems. This environment is independent of the flight hardware that will eventually host the flight software, making it possible to develop the software simultaneously with, or even before, the hardware is delivered. Optionally, by use of interfaces included in VirtualSat, hardware can be used instead of simulated. The flight software, coded in the C or C++ programming language, is compilable and loadable into VirtualSat without any special modifications. Thus, VirtualSat can serve as a relatively inexpensive software test-bed for development test, integration, and post-launch maintenance of spacecraft flight software.

*This program was written by Stephan R. Hammers of the Hammers Co., Inc. for Goddard Space Flight Center. Further information is contained in a TSP (see page 1). GSC-14824-1*

---

### Small-Body Extensions for the Satellite Orbit Analysis Program (SOAP)

An extension to the SOAP software allows users to work with tri-axial ellipsoid-based representations of planetary bodies, primarily for working with small, natural satellites, asteroids, and comets. SOAP is a widely used tool for the visualization and analysis of space missions. The small body extension provides the same

visualization and analysis constructs for use with small bodies. These constructs allow the user to characterize satellite path and instrument cover information for small bodies in both 3D display and numerical output formats.

Tri-axial ellipsoids are geometric shapes the diameters of which are different in each of three principal  $x$ ,  $y$ , and  $z$  dimensions. This construct provides a better approximation than using spheres or oblate spheroids (ellipsoids comprising two common equatorial diameters as a distinct polar diameter). However, the tri-axial ellipsoid is considerably more difficult to work with from a modeling perspective. In addition, the SOAP small-body extensions allow the user to actually employ a plate model for highly irregular surfaces. Both tri-axial ellipsoids and plate models can be assigned to coordinate frames, thus allowing for the modeling of arbitrary changes to body orientation.

A variety of features have been extended to support tri-axial ellipsoids, including the computation and display of the spacecraft sub-orbital point, ground trace, instrument footprints, and swathes. Displays of 3D instrument volumes can be shown interacting with the ellipsoids. Longitude/latitude grids, contour plots, and texture maps can be displayed on the ellipsoids using a variety of projections. The distance along an arbitrary line of sight can be computed between the spacecraft and the ellipsoid, and the coordinates of that intersection can be plotted as a function of time. The small-body extension supports the same visual and analytical constructs that are supported for spheres and oblate spheroids in SOAP making the implementation of the more complex algorithms largely transparent to the user.

*This work was done by Robert Carnright of Caltech and David Stodden and John Coggi of The Aerospace Corporation for NASA's Jet Propulsion Laboratory.*

*This software is available for commercial licensing. Please contact Karina Edmonds of the California Institute of Technology at (626) 395-2322. Refer to NPO-45054.*

---

### Scripting Module for the Satellite Orbit Analysis Program (SOAP)

This add-on module to the SOAP software can perform changes to simulation objects based on the occurrence of specific conditions. This allows the software to encompass simulation response of

scheduled or physical events. Users can manipulate objects in the simulation environment under programmatic control. Inputs to the scripting module are Actions, Conditions, and the Script. Actions are arbitrary modifications to constructs such as Platform Objects (i.e. satellites), Sensor Objects (representing instruments or communication links), or Analysis Objects (user-defined logical or numeric variables). Examples of actions include changes to a satellite orbit ( $v$ ), changing a sensor-pointing direction, and the manipulation of a numerical expression. Conditions represent the circumstances under which Actions are performed and can be couched in If-Then-Else logic, like performing  $v$  at specific times or adding to the spacecraft power only when it is being illuminated by the Sun.

The SOAP script represents the entire set of conditions being considered over a specific time interval. The output of the scripting module is a series of events, which are changes to objects at specific times. As the SOAP simulation clock runs forward, the scheduled events are performed. If the user sets the clock back in time, the events within that interval are automatically undone.

This script offers an interface for defining scripts where the user does not have to remember the vocabulary of various keywords. Actions can be captured by employing the same user interface that is used to define the objects themselves. Conditions can be set to invoke Actions by selecting them from pull-down lists. Users define the script by selecting from the pool of defined conditions. Many space systems have to react to arbitrary events that can occur from scheduling or from the environment. For example, an instrument may cease to draw power when the area that it is tasked to observe is not in view. The contingency of the planetary body blocking the line of sight is a condition upon which the power being drawn is set to zero. It remains at zero until the observation objective is again in view. Computing the total power drawn by the instrument over a period of days or weeks can now take such factors into consideration. What makes the architecture especially powerful is that the scripting module can look ahead and behind in simulation time, and this temporal versatility can be leveraged in displays such as  $x$ - $y$  plots. For example, a plot of a satellite's altitude as a function of time can take changes to the orbit into account.

*This work was done by Robert Carnright of Caltech and David Stodden, John Coggi, and*

*Jim Paget of The Aerospace Corporation for NASA's Jet Propulsion Laboratory.*

*This software is available for commercial licensing. Please contact Karina Edmonds of the California Institute of Technology at (626) 395-2322. Refer to NPO-45055.*

---

### XML-Based SHINE Knowledge Base Interchange Language

The SHINE Knowledge Base Interchange Language software has been designed to more efficiently send new knowledge bases to spacecraft that have been embedded with the Spacecraft Health Inference Engine (SHINE) tool. The intention of the behavioral model is to capture most of the information generally associated with a spacecraft functional model, while specifically addressing the needs of execution within SHINE and Livingstone. As such, it has some constructs that are based on one or the other.

As NASA/JPL autonomous science missions go deeper and deeper into space, the collection of unexpected data becomes a problem. Data structures can easily be implemented in advance that can collect any kind of data; however, when it comes to processing the data into information and taking advantage of serendipitous science discovery, designing a fixed and efficient data structure becomes increasingly complex. This software defines and implements a new kind of data structure that can be used for representing information that is derived from serendipitous data discovery. It allows the run-time definition of arbitrarily complex structures that can adapt at run-time as the raw science data is transformed into information.

This solves the problem decision trees can be prone to, namely how expensive they can be to execute because of the need to evaluate each non-leaf node and, based upon its truth, to either progress deeper into the structure or to examine an alternative. This requires many machine cycles, which can negatively affect time-critical decisions.

This software runs on a variety of different platforms, including SUN, HP, Intel, Apple Macs, Flight Processors, etc. It can be distributed in either source code or binary code and requires a LISP compiler to run with a number, such compilers being either commercially available or found as shareware. The software has no specific memory requirements and depends on the applications that are running in it. It is implemented

as a library package and folds into whatever environment is calling it.

Currently, this software is a component of the Common Automation Engine (CAE) that was developed for Deep Space Network (DSN). It has been in active use for over three years and has been installed in a shadow mode running at Goldstone and DSN monitoring operations at JPL.

*This work was done by Mark James, Ryan Mackey, and Raffi Tikidjian of Caltech for NASA's Jet Propulsion Laboratory. Further information is contained in a TSP (see page 1).*

*This software is available for commercial licensing. Please contact Karina Edmonds of the California Institute of Technology at (626) 395-2322. Refer to NPO-44546.*

---

### Core Technical Capability Laboratory Management System

The Core Technical Capability Laboratory Management System (CTCLMS) consists of dynamically generated Web pages used to access a database containing detailed CTC lab data with the software hosted on a server that allows users to have remote access. Users log into the system with their KSC (or other domain) username and password. They are authenticated within that domain and their CTCLMS user privileges are then authenticated within the system. Based on the different user's privileges (roles), menu options are displayed. CTCLMS users are assigned roles such as Lab Member, Lab Manager, Natural Neighbor Integration Manager, Organizational Manager, CTC Program Manager, or Administrator. The role assigned determines the users' capabilities within the system. Users navigate the menu to view, edit, modify or delete laboratory and equipment data, generate financial and managerial reports, and perform other CTC lab-related functions and analyses.

High availability and detail of lab data gives management insight into the needs and requirements of KSC CTC-funded labs. Comprehensive, quantitative, current data are available in one easily accessible location for Program Operating Plan (POP) development, justification of POP submittals, overguide requests, contract renewals, and phasing of maintenance and replacement requirements. Lab health is quantitatively understandable. Financial and managerial reports are generated automatically from detailed data, and facilitate uniform com-

parison and assessment of lab requirements. Budgets and program estimates are based on empirical data.

Features of the system include addition, modification, deletion, and viewing of lab hardware and software equipment data. Equipment data include equipment name, type, description, manufacturer, and other key parameters. CTCLMS also prioritizes obsolete equipment replacement at three levels of responsibility, manages the addition of new users and the assignment of roles and submits current lab conditions and costs.

*This work was done by Linda Shaykhian, Curtis Dugger, and Laurie Griffin for Kennedy Space Center. Further information is contained in a TSP (see page 1). KSC-13051*

---

### **MRO SOW Daily Script**

The MRO SOW daily script (wherein “MRO” signifies “Mars Reconnaissance Orbiter” and “SOW” signifies “sequence systems engineer of the week”) is a computer program that automates portions of the MRO daily SOW proce-

dures, which includes checking file-system sizes and automated sequence processor (ASP) log files. The MRO SOW daily script effects clear reporting of (1) the status of, and requirements imposed on, the file system and (2) the ASP log files.

*This program was written by Forest W. Fisher, Teerapat Khanampornpan, and Roy E. Gladden of Caltech for NASA's Jet Propulsion Laboratory.*

*This software is available for commercial licensing. Please contact Karina Edmonds of the California Institute of Technology at (626) 395-2322. Refer to NPO-45439.*



## Tool for Inspecting Alignment of Twinaxial Connectors

Misalignment can be detected before damage is done.

Lyndon B. Johnson Space Center, Houston, Texas

A proposed tool would be used to inspect alignments of mating twinaxial-connector assemblies on interconnecting wiring harnesses. More specifically, the tool would be used to inspect the alignment of each contact pin of each connector on one assembly with the corresponding socket in the corresponding connector on the other assembly. It is necessary to inspect the alignment because if mating of the assemblies is attempted when any pin/socket pair is misaligned beyond tolerance, the connection will not be completed and the dielectric material in the socket will be damaged (see Figure 1).

Although the basic principle of the tool is applicable to almost any type of mating connector assemblies, the specific geometry of the tool must match the pin-and-socket geometry of the specific mating assemblies to be inspected. In the original application for which the tool was conceived, each of the mating assemblies contains eight twinaxial connectors; the pin diameter is 0.014 in. ( $\approx 0.35$  mm), and the maximum allowable pin/socket misalignment is 0.007 in. ( $\approx 0.18$  mm). Incomplete connections can result in loss of flight data within the functional path to the space-shuttle crew cockpit displays.

The tool (see Figure 2) would consist mainly of a transparent disk with alignment clocking tabs that can be fitted



Figure 1. The Dielectric Material Near Sockets is damaged in two of the connectors shown here, because of an attempt to mate them with connectors containing pins that were misaligned with the sockets.

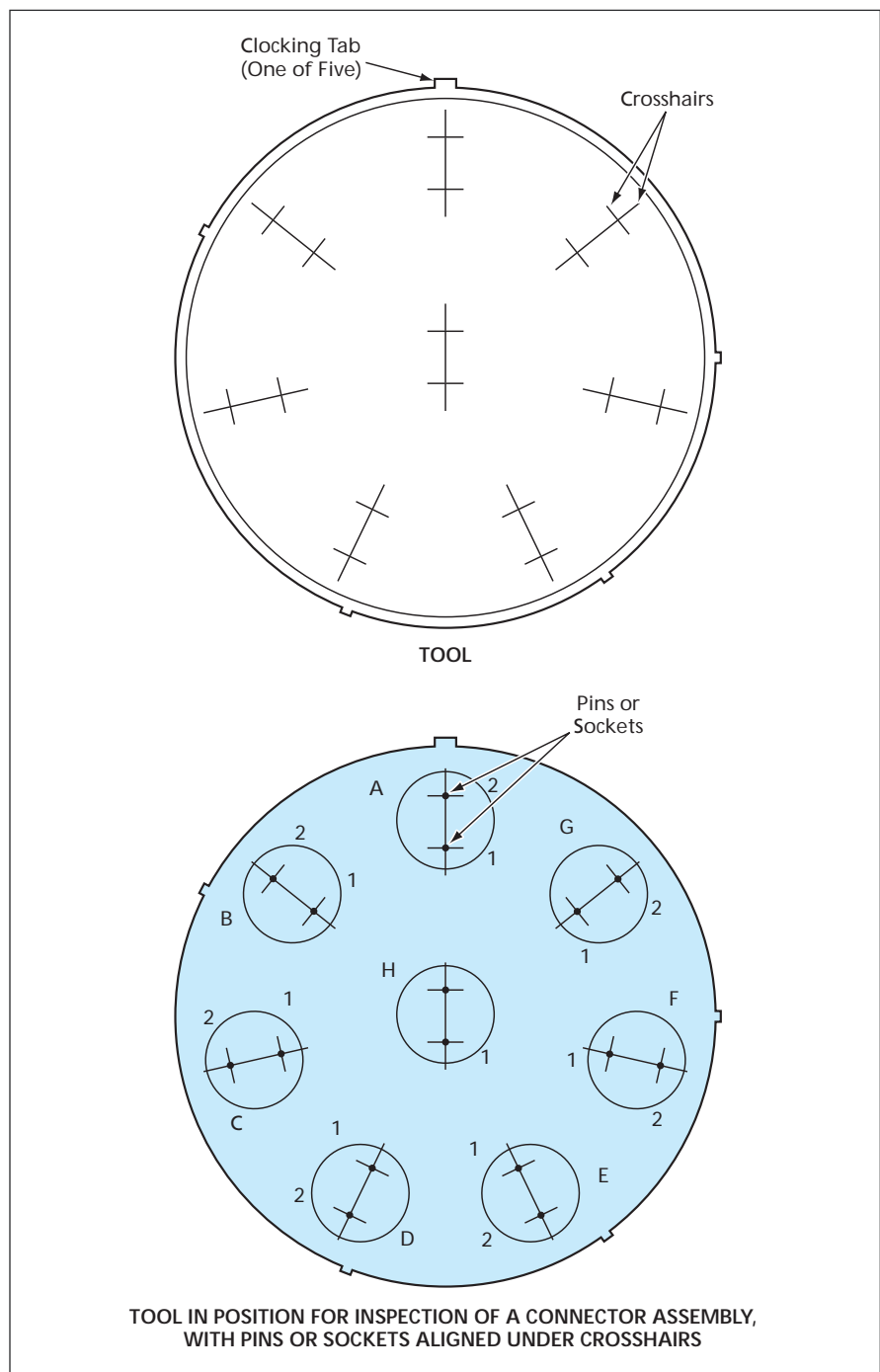


Figure 2. The **Inspection Tool** would contain a reticle sized and shaped specifically for the connector assembly to be inspected. The tool would be fit onto the connector assembly. Misalignments would be readily apparent as deviations of pin or socket locations within circles.

onto either connector assembly. Sets of circles or equivalent reference markings are affixed to the face of the tool, located at the desired positions of the mating contact pairs. An inspector would simply fit the tool onto a connector assembly, engaging the clocking tabs until the tool fits tightly. The inspector would then align one set of cir-

cles positioning a line of sight perpendicular to one contact within the connector assembly. Misalignments would be evidenced by the tip of a pin contact straying past the inner edge of the circle. Socket contact misalignments would be evidenced by a crescent-shaped portion of the white dielectric appearing within the circle. The tool

could include a variable magnifier plus an illuminator that could be configured so as not to cast shadows.

*This work was done by Christopher R. Smith of United Space Alliance for Johnson Space Center. For further information, contact the Johnson Commercial Technology Office at (281) 483-3809. MSC-23757*

---

## ⚙️ An ATP System for Deep-Space Optical Communication

*NASA's Jet Propulsion Laboratory, Pasadena, California*

An acquisition, tracking, and pointing (ATP) system is proposed for aiming an optical-communications downlink laser beam from deep space. In providing for a direction reference, the concept exploits the mature technology of star trackers to eliminate the need for a costly and potentially hazardous laser beacon. The system would include one optical and two inertial sensors, each contributing primarily to a different portion of the frequency spectrum of the pointing signal: a star

tracker (<10 Hz), a gyroscope (<50 Hz), and a precise fluid-rotor inertial angular-displacement sensor (sometimes called, simply, "angle sensor") for the frequency range >50 Hz. The outputs of these sensors would be combined in an iterative averaging process to obtain high-bandwidth, high-accuracy pointing knowledge. The accuracy of pointing knowledge obtainable by use of the system was estimated on the basis of an 8-cm-diameter telescope and known parameters of com-

mercially available star trackers and inertial sensors: The single-axis pointing-knowledge error was found to be characterized by a standard deviation of 150 nanoradians — below the maximum value (between 200 and 300 nanoradians) likely to be tolerable in deep-space optical communications.

*This work was done by Shinhak Lee, Gerardo Ortiz, and James Alexander of Caltech for NASA's Jet Propulsion Laboratory. For more information, contact [iaoffice@jpl.nasa.gov](mailto:iaoffice@jpl.nasa.gov). NPO-41736*

---

## ⚙️ Polar Traverse Rover Instrument

*NASA's Jet Propulsion Laboratory, Pasadena, California*

A Polar Traverse Rover (PTR) is a device designed to determine the role of Antarctica in the global climate system by determining typical paths of continental air that passes the South Pole, and by obtaining insight into the relationship between events at the Antarctic and the meteorology of sub-polar altitudes. The PTR is a 2-m-diameter ball in which an Iridium modem, with an integrated global positioning system (GPS) receiver and a commercial lithium battery pack, is suspended. The modem is

attached to an aluminum plate and is surrounded by shock-absorbing plastic for protection. This core is attached to the interior walls of the shell by strings on three axis points. The unit's total weight is 10 kg, and it returns data regarding location, altitude, ground velocity, and vertical velocity.

The PTR traverses the terrain solely through being blown around by the wind. The unit is much lighter than its predecessor, the Tumbleweed, and requires less wind to put it in motion and to sustain mo-

tion. The system is autonomous, requiring minimal monitoring, and enables long-range, unmanned scientific surface surveys in harsh environments.

*This work was done by Alberto Behar of Caltech; Henrik Karlsson and Andreea Radulescu of International Space University; Jonas Jonsson of Angstrom Space Laboratory; and Mika Pegors, Spacegrant Student for NASA's Jet Propulsion Laboratory. For more information, contact [iaoffice@jpl.nasa.gov](mailto:iaoffice@jpl.nasa.gov). NPO-45463*



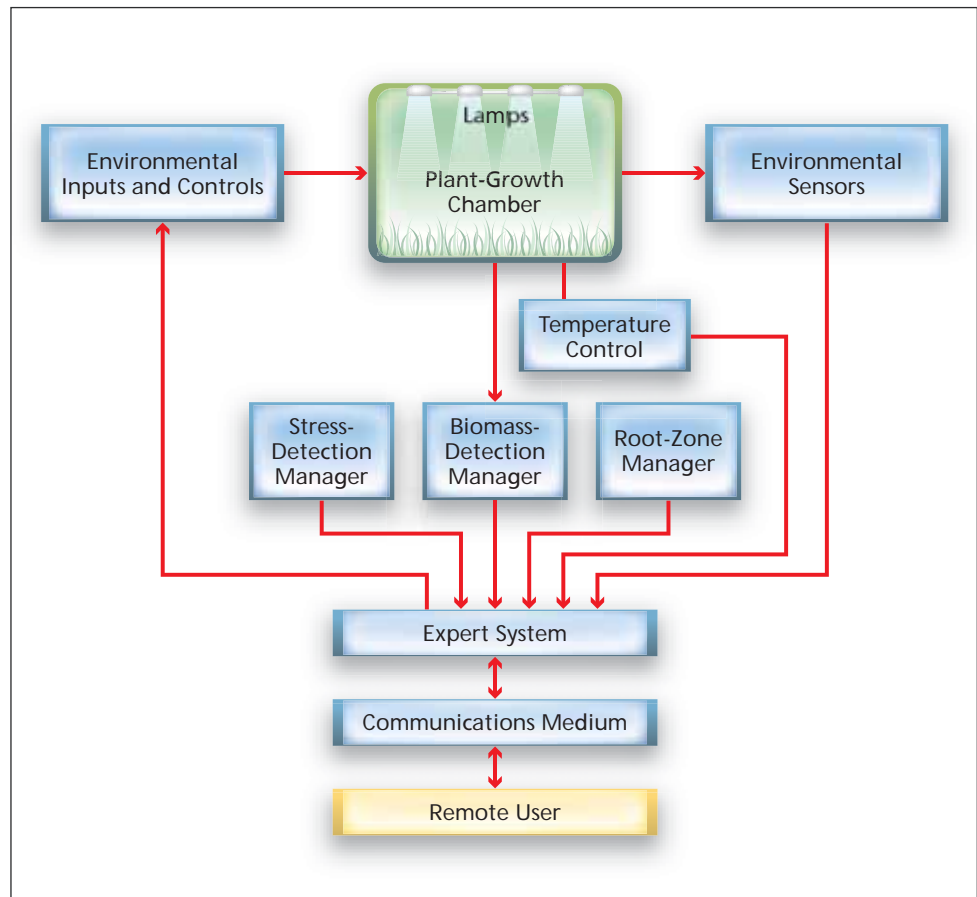
## Expert System Control of Plant Growth in an Enclosed Space

An adjustable environment optimizes growth while minimizing consumption of resources.

*Stennis Space Center, Mississippi*

The Expert System is an enclosed, controlled environment for growing plants, which incorporates a computerized, knowledge-based software program that is designed to capture the knowledge, experience, and problem-solving skills of one or more human experts in a particular discipline. The Expert System is trained to analyze crop/plant status, to monitor the condition of the plants and the environment, and to adjust operational parameters to optimize the plant-growth process. This system is intended to provide a way to remotely control plant growth with little or no human intervention. More specifically, the term “control” implies an autonomous method for detecting plant states such as health (biomass) or stress and then for recommending and implementing cultivation and/or remediation to optimize plant growth and to minimize consumption of energy and nutrients. Because of difficulties associated with delivering energy and nutrients remotely, a key feature of this Expert System is its ability to minimize this effort and to achieve optimum growth while taking into account the diverse range of environmental considerations that exist in an enclosed environment.

The plant-growth environment for the Expert System could be made from a variety of structures, including a greenhouse, an underground cavern, or another enclosed chamber. Imaging equipment positioned within or around the chamber provides spatially distributed crop/plant-growth information. Sensors mounted in the chamber provide data and information pertaining to environmental conditions that could affect plant development. Lamps in the growth environment structure supply illumination, and other additional equipment in the chamber supplies essential nutrients and chemicals. The illumination is also designed to support plant-health imaging di-



The Expert System adjusts inputs in response to image data and other sensory data, and controls the environment so that optimum plant-growth conditions are maintained.

agnostics. Real-time data collected from the various devices enable monitoring capabilities. The Expert System processes the information provided by the imaging and sensor subsystems (see figure). In response, the spatial and temporal patterns of light and the supply of nutrients adjust to maintain optimal performance. The system includes a communication link to a remotely located user via a distant interface, so that the Expert System is accessible and activity within the growth chamber can be assessed and/or overridden when and if necessary. Future applications of the Expert System include biopharming technological applications on Earth and bioregenerative Advanced Life Sup-

port Systems in space.

*This work was done by George May, Mark Lanoue, and Matthew Bethel of the Institute for Technology Development and Robert E. Ryan of Science Systems and Applications, Inc., for Stennis Space Center.*

*Inquiries concerning rights for the commercial use of this invention should be addressed to:*

*Institute for Technology Development*

*Building 1103, Suite 118*

*Stennis Space Center, MS 39529*

*Phone No.: (228) 688-2509*

*E-mail: gmay@iftd.org*

*Refer to SSC-00258, volume and number of this NASA Tech Briefs issue and the page number.*

# Detecting Phycocyanin-Pigmented Microbes in Reflected Light

Concentrations are estimated from ratios between spectral radiances.

John H. Glenn Research Center, Cleveland, Ohio

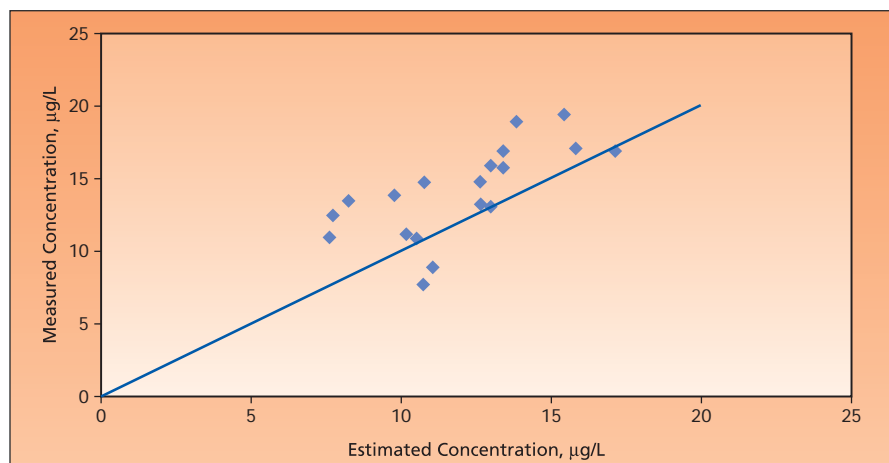
A recently invented method of measuring concentrations of phycocyanin-pigmented algae and bacteria in water is based on measurement of the spectrum of reflected sunlight. When present in sufficiently high concentrations, phycocyanin-pigmented microorganisms can be hazardous to the health of humans who use, and of animals that depend on, an affected body of water. The present method is intended to satisfy a need for a rapid, convenient means of detecting hazardous concentrations of phycocyanin-pigmented microorganisms. Rapid detection will speed up the issuance of public health warnings and performance of corrective actions.

The method involves the measurement of light reflected from a body of water in at least two, but preferably five wavelength bands. In one version of the method, the five wavelength bands are bands 1, 3, 4, 5, and 7 of the Thematic Mapper (TM) multispectral imaging instrument aboard the Landsat-7 satellite (see table). In principle, other wavelength bands indicative of phycocyanin could be used alternatively or in addition to these five. Moreover, although the method was originally intended specifically for processing Landsat-7 TM data, it is equally applicable to processing of data from other satellite-borne instruments or from airborne, hand-held, buoy-mounted, tower-mounted, or otherwise mounted instruments that measure radiances of light reflected from water in the wavelength bands of interest.

The radiance measurements are digitized and used to estimate the concentration of phycocyanin-pigmented microbes by means of the equation  $X = K_1 - K_2R_{31} + K_3R_{41} - K_4R_{43} - K_5R_{53} + K_6R_{73} - K_7R_{74}$ , where  $X$  is the approximate concentration of phycocyanin-pigmented

Band Index	Approximate Lower Wavelength Limit, $\mu\text{m}$	Approximate Upper Wavelength Limit, $\mu\text{m}$
1	0.45	0.52
3	0.63	0.69
4	0.76	0.90
5	1.55	1.75
7	2.08	2.35

Reflected Light in These Wavelength Bands is measured, and the measurements are used to estimate concentrations of phycocyanin-pigmented microbes in water.



Measured Concentrations of Phycocyanin in water samples (represented by the dots) collected from Lake Erie on September 27, 2000 are compared with concentration estimated by means of the equation in the text (represented by the straight line) incorporating  $K_i$  values obtained by correlation with water-sample concentrations measured on July 1, 2000.

microbes; for any pair of band indices  $i$  and  $j$ ,  $R_{ij}$  is the radiance in band  $i$  divided by the radiance in band  $j$ , calculated after subtraction for atmospheric haze in each band; and the  $K_i$  values are chosen to obtain the best correlation between the estimated concentrations and concentrations determined by laboratory analysis of water samples. The figure presents an example of concentrations estimated from a set of Landsat data by use of this equation and the cor-

responding concentrations determined from water samples.

*This work was done by Robert K. Vincent of Bowling Green State University for Glenn Research Center. Further information is contained in a TSP (see page 1).*

*Inquiries concerning rights for the commercial use of this invention should be addressed to NASA Glenn Research Center, Innovative Partnerships Office, Attn: Steve Fedor, Mail Stop 4-8, 21000 Brookpark Road, Cleveland, Ohio 44135. Refer to LEW-18202-1.*



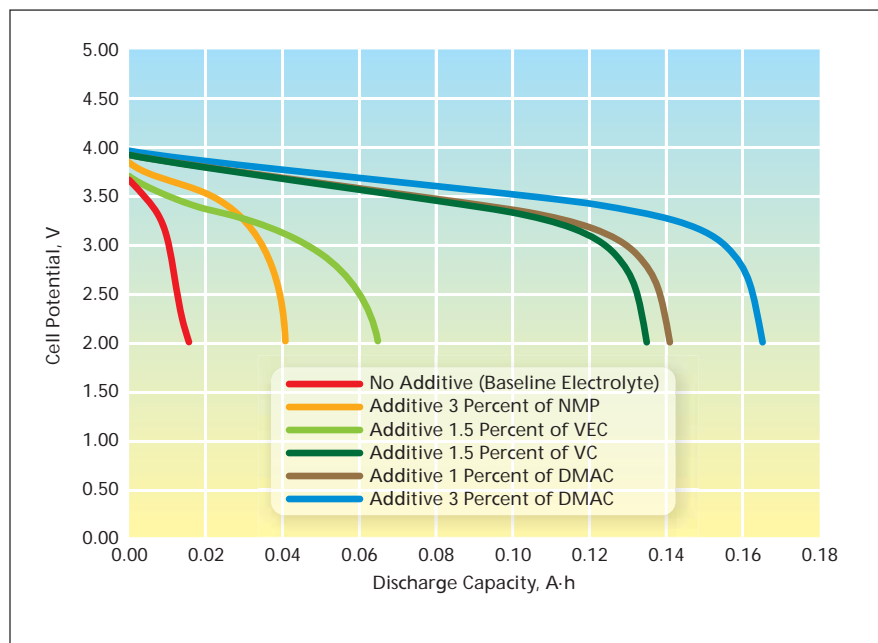
## DMAC and NMP as Electrolyte Additives for Li-Ion Cells High-temperature resilience is increased.

NASA's Jet Propulsion Laboratory, Pasadena, California

Dimethyl acetamide (DMAC) and N-methyl pyrrolidinone (NMP) have been found to be useful as high-temperature-resilience-enhancing additives to a baseline electrolyte used in rechargeable lithium-ion electrochemical cells. The baseline electrolyte, which was previously formulated to improve low-temperature performance, comprises  $\text{LiPF}_6$  dissolved at a concentration of 1.0 M in a mixture comprising equal volume proportions of ethylene carbonate, diethyl carbonate, and dimethyl carbonate. This and other electrolytes comprising lithium salts dissolved in mixtures of esters (including alkyl carbonates) have been studied in continuing research directed toward extending the lower limits of operating temperatures and, more recently, enhancing the high-temperature resilience of such cells. This research at earlier stages, and the underlying physical and chemical principles, were reported in numerous previous *NASA Tech Briefs* articles.

Although these electrolytes provide excellent performance at low temperatures (typically as low as  $-40^\circ\text{C}$ ), when the affected Li-ion cells are subjected to high temperatures during storage and cycling, there occur irreversible losses of capacity accompanied by power fade and deterioration of low-temperature performance. The term "high-temperature resilience" signifies, loosely, the ability of a cell to resist such deterioration, retaining as much as possible of its initial charge/discharge capacity during operation or during storage in the fully charged condition at high temperature. For the purposes of the present development, a temperature is considered to be high if it equals or exceeds the upper limit (typically,  $30^\circ\text{C}$ ) of the operating-temperature range for which the cells in question are generally designed.

Prior studies focusing on the reactivity of electrolytes like the ones of interest here had established that  $\text{LiPF}_6$  can thermally decompose to form  $\text{LiF}$  and  $\text{PF}_5$ , the later product being a strong Lewis acid that further reacts with alkyl carbonates to form a number of byprod-



Reversible Capacities, after storage at a temperature of  $65^\circ\text{C}$  of cells containing the baseline electrolyte plus various additives were measured at  $20^\circ\text{C}$  at a discharge rate of 25 mA [numerically equal to 1/16 of (the nominal capacity in A-h)] after the cells had been charged to a potential of 4.1 V at a rate of 25 mA.

ucts. The present additives — DMAC and NMP — are Lewis bases that act as stabilizing agents in that they reversibly bind with  $\text{PF}_5$ , thereby preventing decomposition of the carbonate solvents at high temperature.

To enable testing of these additives, rechargeable carbon-anode/ $\text{LiNi}_{0.8}\text{Co}_{0.2}\text{O}_2$ -cathode cells containing the baseline electrolyte plus various proportions of these additives were assembled. For comparison, cells containing, variously, the baseline electrolyte alone or the baseline electrolyte plus either of two previously known additives [vinylene carbonate (VC) and vinyl ethylene carbonate (VEC)] were also assembled. The cells were subjected to charge-discharge cycling tests and other electrochemical tests at various temperatures from room temperature ( $23^\circ\text{C}$ ) down to  $-20^\circ\text{C}$ . The cells were also evaluated with respect to high-temperature resilience by measuring the capacities retained after storage for 10 days at a temperature of  $55^\circ\text{C}$ , followed by 10 days at  $60^\circ\text{C}$ , followed by 10

days at  $65^\circ\text{C}$ . The greatest retention of capacity was observed in a cell containing 3 percent of DMAC as the additive. Other cells, in order of decreasing retained capacity, included those containing 1 percent of DMAC, 1.5 percent of VC, 1.5 percent of VEC, 3 percent of NMP, and no additive (see figure).

*This work was done by Marshall Smart and Ratnakumar Bugga of Caltech and Brett Lucht of the University of Rhode Island for NASA's Jet Propulsion Laboratory. Further information is contained in a TSP (see page 1).*

*In accordance with Public Law 96-517, the contractor has elected to retain title to this invention. Inquiries concerning rights for its commercial use should be addressed to:*

*Innovative Technology Assets Management  
JPL*

*Mail Stop 202-233  
4800 Oak Grove Drive  
Pasadena, CA 91109-8099*

*E-mail: iaoffice@jpl.nasa.gov*

*Refer to NPO-44805, volume and number of this NASA Tech Briefs issue, and the page number.*

# Mass Spectrometer Containing Multiple Fixed Collectors

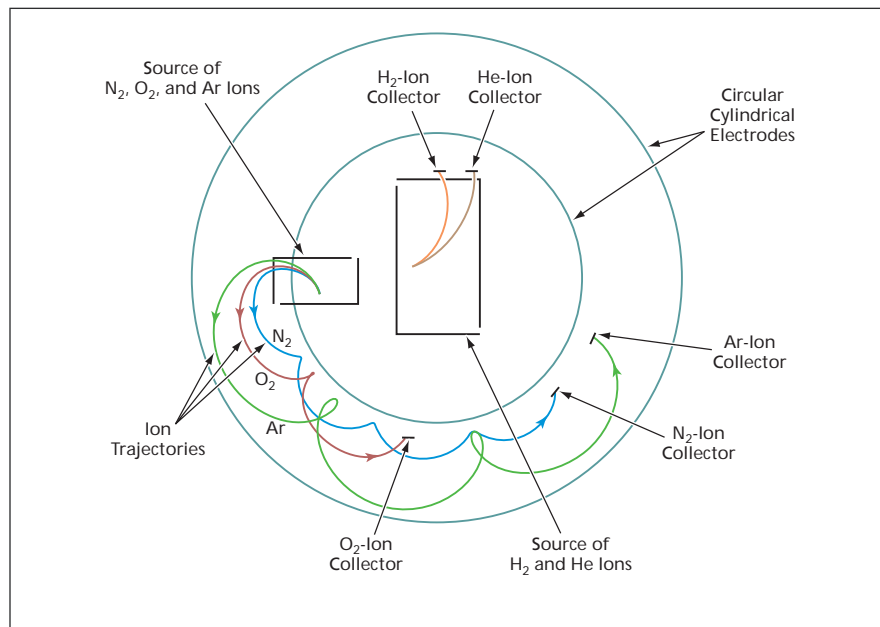
Two mass analyzers in a compact package detect five ion species simultaneously.

John F. Kennedy Space Center, Florida

A miniature mass spectrometer that incorporates features not typically found in prior mass spectrometers is undergoing development. This mass spectrometer is designed to simultaneously measure the relative concentrations of five gases ( $H_2$ , He,  $N_2$ ,  $O_2$ , and Ar) in air, over the relative-concentration range from  $10^{-6}$  to 1, during a sampling time as short as 1 second. It is intended to serve as a prototype of a product line of easy-to-use, portable, lightweight, high-speed, relatively inexpensive instruments for measuring concentrations of multiple chemical species in such diverse applications as detecting explosive or toxic chemicals in air, monitoring and controlling industrial processes, measuring concentrations of deliberately introduced isotopes in medical and biological investigations, and general environmental monitoring.

The heart of this mass spectrometer is an integral combination of a circular cycloidal mass analyzer, multiple fixed ion collectors, and two mass-selective ion sources. By "circular cycloidal mass analyzer" is meant an analyzer that includes (1) two concentric circular cylindrical electrodes for applying a radial electric field and (2) a magnet arranged to impose a magnetic flux aligned predominantly along the cylindrical axis, so that ions, once accelerated into the annulus between the electrodes, move along circular cycloidal trajectories. As in other mass analyzers, trajectory of each ion is determined by its mass-to-charge ratio, and so ions of different species can be collected simultaneously by collectors (Faraday cups) at different locations intersected by the corresponding trajectories (see figure). Unlike in other mass analyzers, the installation of additional collectors to detect additional species does not necessitate increasing the overall size of the analyzer assembly.

Each of the two mass-selective ion sources consists mainly of a filament and electrodes. One of the electrodes is an anode that contains one or more hole(s) through which ions leave the source. The filament, electrodes, and hole(s) are arranged such that under the influence of the combination of electric and magnetic fields, only ions in a desired mass/charge range can leave the source. One of the sources has a single hole



In the Circular Cycloidal Mass Analyzer, ions of  $O_2$ ,  $N_2$ , and Ar follow different trajectories and, hence, can be collected simultaneously at different locations. Another ion-source/analyzer assembly located inside the inner cylindrical electrode generates and detects ions of  $H_2$  and He only.

through which ions in the mass/charge range that includes  $O_2$ ,  $N_2$ , and Ar ions can be released into the annulus between the inner and outer electrodes of the circular cycloidal mass analyzer, wherein collectors for the  $O_2$ ,  $N_2$ , and Ar ions are located.

The other source has two holes — one for  $H_2$  and one for He ions. In the presence of the magnetic field, this source is sufficiently mass-selective that the circular cycloidal mass analyzer is not needed for detecting  $H_2$  and He ions. Therefore, this source is placed, along with collectors facing its two exit holes, within the inner cylindrical electrode, where there is no applied electric field but the applied magnetic field is present. Hence, the combination of this source and its two collectors is characterized as a mass analyzer within a mass analyzer.

The vacuum inside the mass spectrometer is provided by a combination of an ion pump and a non-evaporable-getter pump. This pump combination is designed to operate in conjunction with a gas-inlet system that includes a gas-permeable fluorinated ethylene-propylene membrane and miniature valves. Along with the operation of the rest of the instrument, operation of the valves and pumps is coordinated by a computer to

ensure that a high vacuum is retained when the instrument is switched off and the ion pump can be restarted safely after a long rest.

Current-to-voltage converters needed for processing the collector outputs are placed within the vacuum, close to the collectors, in order to minimize stray capacitance. Each such converter includes a number of feedback resistors for different sensitivity ranges. Special miniature, highly insulated, leaf-spring switches actuated by current pulses in the presence of the applied magnetic field have been developed to satisfy the unique combination of requirements for switching among the different feedback resistors.

*This work was done by Robert Moskala, Alan Celo, Guenter Voss, and Tom Shaffer of Monitor Instruments Co., LLC for Kennedy Space Center.*

*In accordance with Public Law 96-517, the contractor has elected to retain title to this invention. Inquiries concerning rights for its commercial use should be addressed to:*

*Monitor Instruments Co., LLC  
290 East Union Road  
Cheswick, PA 15024-2107*

*Refer to KSC-12793/936, volume and number of this NASA Tech Briefs issue, and the page number.*

---

## Waveguide Harmonic Generator for the SIM

NASA's Jet Propulsion Laboratory, Pasadena, California

A second-harmonic generator (SHG) serves as the source of the visible laser beam in an onboard calibration scheme for NASA's planned Space Interferometry Mission (SIM), which requires an infrared laser beam and a visible laser beam coherent with the infrared laser beam. The SHG includes quasi-phase-matched waveguides made of MgO-doped, periodically poled lithium niobate, pigtailed with polarization-maintaining optical fibers. Frequency doubling by use of such waveguides affords

the required combination of coherence and sufficient conversion efficiency for the intended application. The spatial period of the poling is designed to obtain quasi-phase-matching at a nominal middle excitation wavelength of 1,319.28 nm.

The SHG is designed to operate at a warm bias (ambient temperature between 20 and 25 °C) that would be maintained in its cooler environment by use of electric heaters; the heater power would be adjusted to regulate

the temperature precisely and thereby maintain the required precision of the spatial period. At the state of development at the time of this reporting, the SHG had been packaged and subjected to most of its planned space-qualification tests.

*This work was done by Daniel Chang, Ilya Poberezhskiy, and Jerry Mulder of Caltech for NASA's Jet Propulsion Laboratory. For more information, contact iaoffice@jpl.nasa.gov. NPO-45253*

---

## Whispering Gallery Mode Resonator With Orthogonally Reconfigurable Filter Function

NASA's Jet Propulsion Laboratory, Pasadena, California

An optical resonator has been developed with reconfigurable filter function that has resonant lines that can be shifted precisely and independently from each other, creating any desirable combination of resonant lines. This is achieved by changing the axial distribution of the effective refractive index of the resonator, which shifts the resonant frequency of particular optical modes, leaving all the rest unchanged. A reconfigurable optical filter is part of

the remote chemical detector proposed for the Mars mission (Planetary Instrument Definition and Development Program — PIDDP), but it is also useful for photonic communications devices.

*This work was done by Lute Maleki, Andrey Matsko, Dmitry Strelakov, and Anatoliy Savchenkov of Caltech for NASA's Jet Propulsion Laboratory.*

*In accordance with Public Law 96-517, the contractor has elected to retain title to*

*this invention. Inquiries concerning rights for its commercial use should be addressed to:*

*Innovative Technology Assets Management  
JPL*

*Mail Stop 202-233*

*4800 Oak Grove Drive*

*Pasadena, CA 91109-8099*

*E-mail: iaoffice@jpl.nasa.gov*

*Refer to NPO-44948, volume and number of this NASA Tech Briefs issue, and the page number.*

---

## Stable Calibration of Raman Lidar Water-Vapor Measurements

Data from occasional radiosonde campaigns and routine laboratory lamp measurements are utilized.

NASA's Jet Propulsion Laboratory, Pasadena, California

A method has been devised to ensure stable, long-term calibration of Raman lidar measurements that are used to determine the altitude-dependent mixing ratio of water vapor in the upper troposphere and lower stratosphere. Because the lidar measurements yield a quantity proportional to the mixing ratio, rather than the mixing ratio itself, calibration is necessary to obtain the factor of proportionality. The present method involves the use of calibration data from two sources: (1) absolute calibration data from *in situ* radiosonde measurements made during occasional campaigns and (2) partial calibration data obtained by use, on a regular schedule, of a lamp that emits in a known spectrum de-

termined in laboratory calibration measurements.

In this method, data from the first radiosonde campaign are used to calculate a campaign-averaged absolute lidar calibration factor ( $t_l$ ) and the corresponding campaign-averaged ratio ( $L_l$ ) between lamp irradiances at the water-vapor and nitrogen channel wavelengths. Depending on the scenario considered, this ratio can be assumed to be either constant over a long time ( $L = L_l$ ) or drifting slowly with time.

The absolutely calibrated water-vapor mixing ratio ( $q$ ) obtained from the  $i$ th routine off-campaign lidar measurement run is given by

$$q_i = P_i / t_i = LP_i / P'_i$$

where  $P_i$  is water-vapor/nitrogen measurement signal ratio,  $t_i$  is the unknown and unneeded overall efficiency ratio of the lidar receiver during the  $i$ th routine off-campaign measurement run, and  $P'_i$  is the water-vapor/nitrogen signal ratio obtained during the lamp run associated with the  $i$ th routine off-campaign measurement run. If  $L$  is assumed constant, then the lidar calibration is routinely obtained without the need for new radiosonde data. In this case, one uses  $L = L_l = P'_1 / t_1$ , where  $P'_1$  is the water-vapor/nitrogen signal ratio obtained during the lamp run associated with the first radiosonde campaign.

If  $L$  is assumed to drift slowly, then it is necessary to postpone calculation of  $q_i$  until after a second radiosonde campaign. In this case, one obtains a new value,  $L_2$ , from the second radiosonde

campaign, and for the  $i$ th routine off-campaign measurement run, one uses an intermediate value of  $L$  obtained by simple linear time interpolation between  $L_1$  and  $L_2$ .

*This work was done by Thierry Leblanc and Iain S. McDermid of Caltech for NASA's Jet Propulsion Laboratory. For more information, contact iaoffice@jpl.nasa.gov. NPO-45955*

## Bimaterial Thermal Compensators for WGM Resonators

Net thermal drifts of spectra would be cancelled to first order.

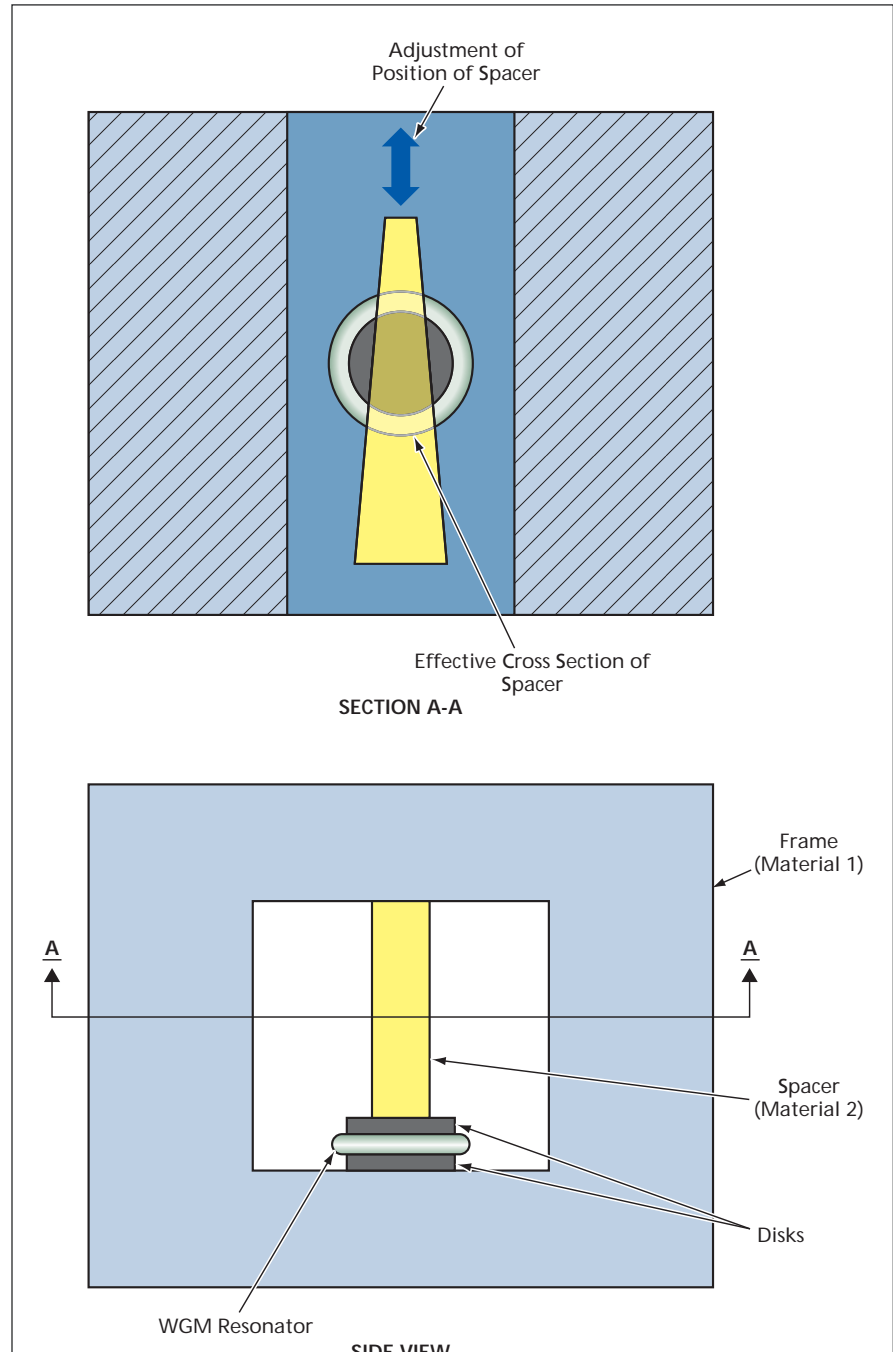
NASA's Jet Propulsion Laboratory, Pasadena, California

Bimaterial thermal compensators have been proposed as inexpensive means of preventing (to first order) or reducing temperature-related changes in the resonance frequencies of whispering-gallery-mode (WGM) optical resonators. A bimaterial compensator would apply, to a WGM resonator, a pressure that would slightly change the shape of the resonator and thereby change its resonance frequencies. Through suitable choice of the compensator dimensions and materials, it should be possible to make the temperature dependence of the pressure-induced frequency shift equal in magnitude and opposite in sign to the temperature dependence of the frequency shift of the uncompensated resonator so that, to first order, a change in temperature would cause zero net change in frequency.

A bimaterial compensator as proposed (see figure) would include (1) a frame made of one material (typically, a metal) having a thermal-expansion coefficient  $\alpha_1$  and (2) a spacer made of another material (typically, a glass) having a thermal-expansion coefficient  $\alpha_2$ . The WGM resonator would be sandwiched between disks and the resulting sandwich would be squeezed between the frame and the spacer (see figure). Assuming that the cross-sectional area of the frame greatly exceeded the cross-sectional area of the spacer and that the thickness of the sandwich was small relative to the length of the spacer, the net variation in a resonance frequency as a function of temperature would be given by

$$df/dT \approx \partial f/\partial T + (\partial f/\partial F) S_2 E_2 (\alpha_2 - \alpha_1)$$

where  $f$  is the resonance frequency,  $T$  is temperature,  $\partial f/\partial T$  is the rate of change of frequency as a function of temperature of the uncompensated resonator,  $\partial f/\partial F$  is the rate of change of frequency as a function of applied force  $F$  at constant temperature,  $S_2$  is the effective cross-sectional area of the



The Bimaterial Compensator would apply a temperature-dependent stress to counteract the temperature dependence of the spectrum of the uncompensated resonator.

spacer, and  $E_2$  is the modulus of elasticity of the spacer.

Through appropriate choice of materials and geometry, one could obtain temperature compensation — that is, one could make  $df/dT \approx 0$ . For example, the effective spacer cross-sectional area for temperature compensation is given by

$$S_2 \approx (\partial f / \partial T) / [(\partial f / \partial F) E_2 (\alpha_1 - \alpha_2)].$$

Because it would be exceedingly difficult to fabricate the spacer to the precise re-

quired cross section, the spacer would have a wedge total cross section extending beyond the disk diameter, so that the effective cross section could be varied by moving the spacer. As part of the process of fabricating the temperature-compensated WGM resonator, the resonator-and-compensator assembly would be installed on a thermoelectric cooler, which would be used to impose an oscillating temperature on the resonator. The resulting synchronous oscillation of the op-

tical spectrum of the resonator would be monitored on an oscilloscope. The position of the spacer would be shifted in small increments until the synchronous oscillations of the spectrum were reduced to zero.

*This work was done by Anatoliy Savchenkov, Nan Yu, Lute Maleki, Vladimir Iltchenko, Andrey Matsko, and Dmitry Strelakov of Caltech for NASA's Jet Propulsion Laboratory. For more information, contact [iaoffice@jpl.nasa.gov](mailto:iaoffice@jpl.nasa.gov). NPO-44441*





## Root Source Analysis/ ValuStream™ — a Methodology for Identifying and Managing Risks

Root sources of uncertainty are taken into account in a rigorous, systematic way.

Marshall Space Flight Center, Alabama

Root Source Analysis (RoSA) is a systems-engineering methodology that has been developed at NASA over the past five years. It is designed to reduce costs, schedule, and technical risks by systematically examining critical assumptions and the state of the knowledge needed to bring to fruition the products that satisfy mission-driven requirements, as defined for each element of the Work (or Product) Breakdown Structure (WBS or PBS). This methodology is sometimes referred to as the ValuStream method, as inherent in the process is the linking and prioritizing of uncertainties arising from knowledge shortfalls directly to the customer's mission driven requirements. RoSA and ValuStream are synonymous terms.

RoSA is not simply an alternate or improved method for identifying risks. It represents a paradigm shift. The emphasis is placed on identifying very specific knowledge shortfalls and assumptions that are the root sources of the risk (the "why"), rather than on assessing the WBS product(s) themselves (the "what"). In so doing RoSA looks forward to anticipate, identify, and prioritize knowledge shortfalls and assumptions that are likely to create significant uncertainties/risks (as compared to Root Cause Analysis, which is most often used to look back to discover what was not known, or was assumed, that caused the failure). Experience indicates that RoSA, with its primary focus on assumptions and the state of the underlying knowledge needed to define, design, build, verify, and operate the products, can identify critical risks that historically have been missed by the usual approaches (i.e., design review process and classical risk identification methods). Further, the methodology answers four critical questions for decision makers and risk managers:

1. What's been included?
2. What's been left out?
3. How has it been validated?
4. Has the real source of the uncertainty/risk been identified, i.e., is the

perceived problem the real problem?

Users of the RoSA methodology have characterized it as a true "bottoms up" risk assessment. The insights gained regarding specific shortfalls (risks) in the underlying knowledge base are particularly important to decision makers in determining the readiness to proceed at major decisional milestones in the lifecycle of a program.

With RoSA the granularity of the assessment is taken to the level where one can see and assess the *driving assumptions and state of the knowledge* on which the program management and engineering rests, relative to specific customer-driven requirements. The methodology uses a knowledge matrix or grid.

The left side of the matrix is the program/project WBS (or PBS), which is the hierarchy of products, created by the designers, that are needed to satisfy mission requirements. The top of the matrix is a Capability Breakdown Structure (CBS), which is a hierarchy of the programmatic and/or technical disciplines, filled by engineers/scientists (termed Functional Discipline Specialists, FDS's), that provide the underlying knowledge needed to bring the product to fruition. The cells of the matrix are the individual knowledge elements needed for mission success. The FDS's assess the current state of the knowledge for each element and identify knowledge shortfalls that could significantly affect attainment of a customer's goals and requirements. These root sources of uncertainties are characterized as specific, *actionable* shortfalls in the analytical tools and databases, and fabrication verification and operations capabilities needed to provide the products that fulfill the customer's expectations. In the process, critical assumptions are also assessed, and standardized, discipline-unique capability readiness level (CRL) scales are used to quantify the readiness levels and to insure consistency. Once identified, these shortfalls and critical assumptions are analyzed in an interactive, multidisciplinary

process that yields prioritized lists of risks and recommended mitigating actions.

Results from a RoSA assessment constitute a basic input into risk-management plans and technology plans and metrics. A part of the process is an interactive session involving both the FDS's (who tend to be technologically conservative) and the designers (who tend to be optimistic). This interaction between the two different perspectives significantly increases the validity of information.

RoSA is useful for identifying risks at any stage of the life cycle of a program or project. It has shown itself to be effective in validating the achievability of requirements and in identifying and prioritizing root sources of uncertainties/risks (i.e., the root sources of unreliability) in hardware/software from definition through design, as well as in fabrication, verification, and operations processes. It offers a truly independent validation of the technology readiness level (TRL) estimates, whether considering heritage hardware, commercial off-the-shelf (COTS), modified off-the-shelf (MOTS), or insertion of a new technology, by comparing TRL estimates made by the designers with the related capability readiness level (CRL) assessments made by the FDS's for the various WBS products. (The TRL cannot be higher than the underlying CRL of the knowledge elements on which the product depends.) Further, it is effective for planning technology programs and managing the associated risks, assessing technology maturation progress and readiness for deployment and for validating the programmatic and technical readiness of organizational capabilities to execute a program or project.

*This work was done by Richard Lee Brown (self-employed consultant) for Marshall Space Flight Center. Inquiries concerning rights for the commercial use of this invention should be addressed to Sammy Nabors, MSFC Commercialization Assistance Lead, at sammy.a.nabors@nasa.gov. Refer to MFS-32316-1.*

---

## ➤ Ensemble: an Architecture for Mission-Operations Software

Several issues are addressed by capitalizing on the Eclipse open-source software framework.

*NASA's Jet Propulsion Laboratory, Pasadena, California*

"Ensemble" is the name of an open architecture for, and a methodology for the development of, spacecraft mission-operations software. Ensemble is also potentially applicable to the development of non-spacecraft mission-operations-type software.

Ensemble capitalizes on the strengths of the open-source Eclipse software and its architecture to address several issues that have arisen repeatedly in the development of mission-operations software: Heretofore, mission-operations application programs have been developed in disparate programming environments and integrated during the final stages of development of missions. The programs have been poorly integrated, and it has been costly to develop, test, and deploy them. Users of each program have been forced to interact with several different graphical user interfaces (GUIs). Also, the strategy typically used in integrating the programs has yielded serial chains of operational software tools of such a nature that during use of a given tool, it has not been possible to gain access to the capabilities afforded by other tools. In contrast, the Ensemble approach offers a low-risk path towards tighter integration of mission-operations software tools.

Ensemble is based on an adaptation of the Eclipse Rich Client Platform (RCP), which is a widely used, readily available, stable, supported software framework for component-based development of application programs. The Eclipse RCP is a set of Java classes that define an architecture for general component-based application programs. New application programs are built on top of the RCP as

a set of components, called plug-ins, that augment and extend its functionality. For example, a mission-activity-planning application program would consist of the RCP plus a set of plug-ins responsible for displaying, editing, and modeling activity plans. Application programs built on top of the RCP also gain access to a variety of such generally applicable capabilities as a help system, an update manager, and an extensible GUI.

In Ensemble, the difficulties of establishing interfaces between different software tools are minimized by developing most of the tools as Eclipse plug-ins. In addition, Ensemble draws upon capabilities provided by the Eclipse RCP to document and enforce interfaces between different components. In some cases, it may not be possible or prudent to develop a tool as an Eclipse Java plug-in. Such a tool can still be integrated with the Ensemble architecture. Development of a general, robust method of integrating non-Eclipse tools with other Ensemble tools is proceeding.

In Ensemble, the Eclipse framework provides a common GUI that can accommodate GUI components from multiple software tools developed by different teams. To the user, the resulting GUI looks as though it belongs to a single such tool while drawing on the resources of many of them. Ensemble provides for a task-oriented GUI that is based heavily upon an Eclipse perspective, which defines which GUI components are visible to a user at a particular time. As a user moves through tasks required for planning mission operations, the user clicks through a set of icons devoted to each task.

The combination of component-based development and a perspective-based GUI facilitates reuse of any software component at multiple stages of the operations process. In the past, a spacecraft-mission plan would be handed from one software tool to the next in a serial fashion. At each step, a single tool would exert exclusive control over the plan. In contrast, Ensemble plug-ins interact as a group with a common model of an evolving spacecraft plan. Each plug-in can contribute to the plan whenever it is necessary, and each plug-in must respond appropriately to modifications made by other plug-ins.

Most mission-operations-software development teams strive to make their software products applicable to multiple missions, but a typical mission does not need all the capabilities provided by a typical such product. To relieve a mission of the burden of maintaining, learning to use, and testing the software functions that it does not need, Eclipse provides for the distribution, to each mission, of only the core RCP plus only those plug-ins that afford the specific capabilities required by that mission.

*This work was done by Jeffrey Norris, Mark Powell, Jason Fox, Kenneth Rabe, and I-Hsiang Shu of Caltech and Michael McCurdy and Alonso Vera of Ames Research Center for NASA's Jet Propulsion Laboratory. Further information is contained in a TSP (see page 1).*

*The software used in this innovation is available for commercial licensing. Please contact Karina Edmonds of the California Institute of Technology at (626) 395-2322. Refer to NPO-41814.*

---

## ➤ Object Recognition Using Feature-and Color-Based Methods

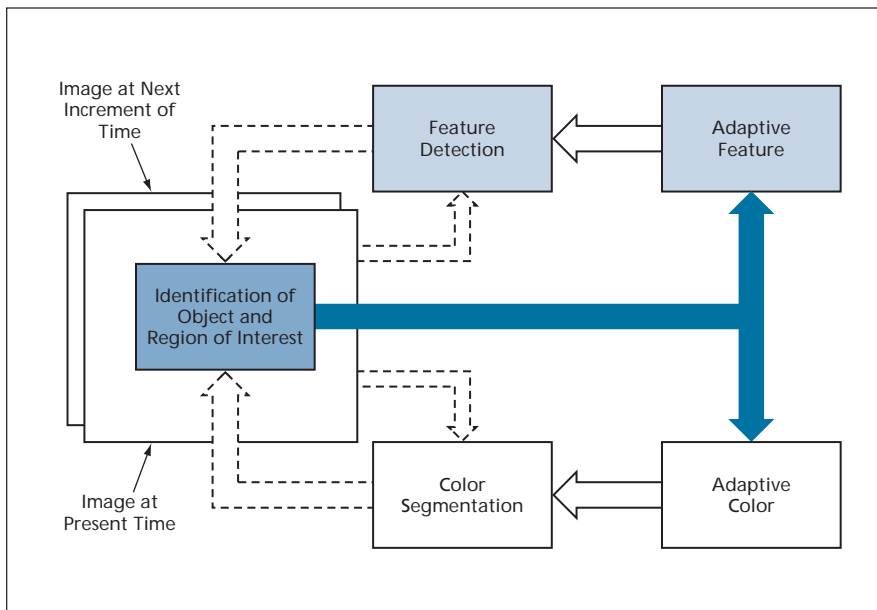
The combination of methods works better than does either method alone.

*NASA's Jet Propulsion Laboratory, Pasadena, California*

An improved adaptive method of processing image data in an artificial neural network has been developed to enable automated, real-time recognition of possibly moving objects under changing (including suddenly changing) conditions of illumination and perspective. The

method involves a combination of two prior object-recognition methods — one based on adaptive detection of shape features and one based on adaptive color segmentation — to enable recognition in situations in which either prior method by itself may be inadequate.

The chosen prior feature-based method is known as adaptive principal-component analysis (APCA); the chosen prior color-based method is known as adaptive color segmentation (ACOSE). These methods are made to interact with each other in a closed-loop system



This **Optimal Adaptive Architecture** involves interaction between a shape-feature-based and a color-segmentation-based method in a cyclic computation. Using shape adaptive features and color adaptive features from the previous cycle, an object and region of interest containing the object are identified in the present image by means of feature detection and color segmentation. The region of interest is then used for sampling data to adapt a new shape and color features for the image during the next cycle.

(see figure) to obtain an optimal solution of the object-recognition problem in a dynamic environment.

One of the results of the interaction is to increase, beyond what would otherwise be possible, the accuracy of the determination of a region of interest (containing an object that one seeks to recognize) within an image. Another re-

sult is to provide a minimized adaptive step that can be used to update the results obtained by the two component methods when changes of color and apparent shape occur. The net effect is to enable the neural network to update its recognition output and improve its recognition capability via an adaptive learning sequence.

In principle, the improved method could readily be implemented in integrated circuitry to make a compact, low-power, real-time object-recognition system. It has been proposed to demonstrate the feasibility of such a system by integrating a 256-by-256 active-pixel sensor with APCA, ACOSE, and neural processing circuitry on a single chip. It has been estimated that such a system on a chip would have a volume no larger than a few cubic centimeters, could operate at a rate as high as 1,000 frames per second, and would consume in the order of milliwatts of power.

*This work was done by Tuan Duong, Vu Duong, and Allen Stubberud of Caltech for NASA's Jet Propulsion Laboratory. Further information is contained in a TSP (see page 1).*

*In accordance with Public Law 96-517, the contractor has elected to retain title to this invention. Inquiries concerning rights for its commercial use should be addressed to:*

*Innovative Technology Assets  
Management*

*JPL*

*Mail Stop 202-233*

*4800 Oak Grove Drive*

*Pasadena, CA 91109-8099*

*(818) 354-2240*

*E-mail: iaoffice@jpl.nasa.gov*

*Refer to NPO-41370, volume and number of this NASA Tech Briefs issue, and the page number.*





### **On-Orbit Multi-Field Wavefront Control With a Kalman Filter**

A document describes a multi-field wavefront control (WFC) procedure for the James Webb Space Telescope (JWST) on-orbit optical telescope element (OTE) fine-phasing using wavefront measurements at the NIRCcam pupil. The control is applied to JWST primary mirror (PM) segments and secondary mirror (SM) simultaneously with a carefully selected ordering. Through computer simulations, the multi-field WFC procedure shows that it can reduce the initial system wavefront error (WFE), as caused by random initial system misalignments within the JWST fine-phasing error budget, from a few dozen  $\mu\text{m}$  to below 50 nm across the entire NIRCcam Field of View, and the WFC procedure is also computationally stable as the Monte-Carlo simulations indicate.

With the incorporation of a Kalman Filter (KF) as an optical state estimator into the WFC process, the robustness of the JWST OTE alignment process can be further improved. In the presence of some large optical misalignments, the Kalman state estimator can provide a reasonable estimate of the optical state, especially for those degrees of freedom that have a significant impact on the system WFE. The state estimate allows for a few corrections to the optical state to

push the system towards its nominal state, and the result is that a large part of the WFE can be eliminated in this step. When the multi-field WFC procedure is applied after Kalman state estimate and correction, the stability of fine-phasing control is much more certain.

Kalman Filter has been successfully applied to diverse applications as a robust and optimal state estimator. In the context of space-based optical system alignment based on wavefront measurements, a KF state estimator can combine all available wavefront measurements, past and present, as well as measurement and actuation error statistics to generate a Maximum-Likelihood optimal state estimator. The strength and flexibility of the KF algorithm make it attractive for use in real-time optical system alignment when WFC alone cannot effectively align the system.

*This work was done by John Lou, Norbert Sigrist, Scott Basinger, and David Redding of Caltech for NASA's Jet Propulsion Laboratory. Further information is contained in a TSP (see page 1). NPO-45793*

### **The Interplanetary Overlay Networking Protocol Accelerator**

A document describes the Interplanetary Overlay Networking Protocol Accelerator (IONAC) — an electronic apparatus, now under development, for

relaying data at high rates in spacecraft and interplanetary radio-communication systems utilizing a delay-tolerant networking protocol. The protocol includes provisions for transmission and reception of data in bundles (essentially, messages), transfer of custody of a bundle to a recipient relay station at each step of a relay, and return receipts.

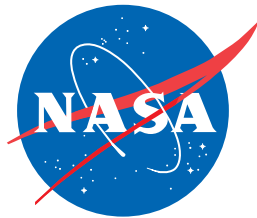
Because of limitations on energy resources available for such relays, data rates attainable in a conventional software implementation of the protocol are lower than those needed, at any given reasonable energy-consumption rate. Therefore, a main goal in developing the IONAC is to reduce the energy consumption by an order of magnitude and the data-throughput capability by two orders of magnitude.

The IONAC prototype is a field-programmable gate array that serves as a reconfigurable hybrid (hardware/firmware) system for implementation of the protocol. The prototype can decode 108,000 bundles per second and encode 100,000 bundles per second. It includes a bundle-cache static random-access memory that enables maintenance of a throughput of 2.7Gb/s, and an Ethernet convergence layer that supports a duplex throughput of 1Gb/s.

*This work was done by Jackson Pang, Jordan L. Torgerson and Loren P. Clare of Caltech for NASA's Jet Propulsion Laboratory. Further information is contained in a TSP (see page 1). NPO-45584*







National Aeronautics and  
Space Administration